LTA for 60 min was not suppressed by treatment with the protein synthesis inhibitor cycloheximide, whereas the release by stimulation with LTA for 4 h was significantly suppressed by the treatment (Fig. 1C). We further investigated whether LTA induction of exocytosis was mediated through MyD88 and IRAK-1, common signaling molecules downstream of TLRs, because LTA is known as a TLR2 agonist. Interestingly, VWF release by stimulation with LTA for 60 min was suppressed by knockdown of the expression of MyD88 but not that of IRAK-1, whereas the release by stimulation with LTA for 4 h was significantly suppressed by each knockdown of MyD88 and IRAK-1 (Fig. 1C). Thus, these results suggest that LTA can induce Weibel-Palade body exocytosis through a MyD88-dependent rapid mechanism without *de novo* protein synthesis and an IRAK-1-dependent slower mechanism with *de novo* protein synthesis.

We also examined whether other bacterial cell wall constituents, as shown in Table 1, activated induction of VWF release after stimulation of HAECs for 60 min. Among the compounds that we tested, the synthetic analogs of bacterial lipoproteins Pam_3CSK_4, FSL-1, and MALP-2 and, to a lesser extent, flagellin induced VWF release in a dose-dependent manner (Fig. 1D, left). Interestingly, LPS from different bacterial species and PGN did not activate Weibel-Palade body exocytosis (Fig. 1D, left). In addition, we found that induction of exocytosis by bacterial compounds was also mediated by MyD88 as well as that by LTA (Fig. 1D, right). These results suggest that several types of, but not all, bacterial cell wall constituents can activate induction of TLR-MyD88-mediated exocytosis.

Regarding the process of Weibel-Palade body exocytosis, we found that MyD88-dependent externalization of P-selectin was induced after stimulation of HAECs with LTA for 30 min (Fig. 2A). In addition, monocyte adhesion to HAECs was modestly increased in a MyD88-dependent fashion after LTA stimulation for 60 min (Fig. 2B).
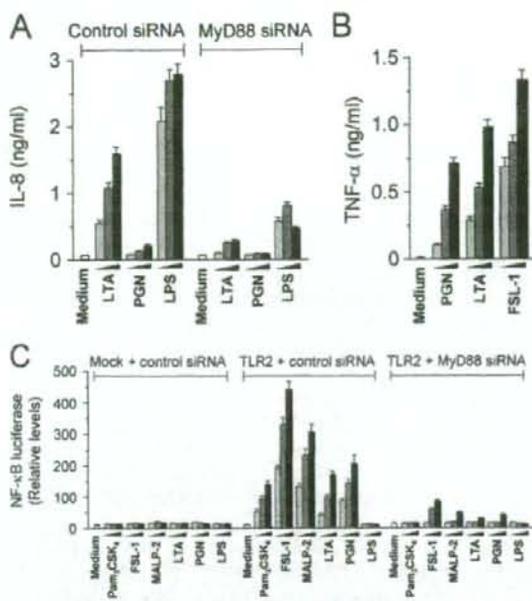
Stimulatory Activities of LPS and PGN in HAECs—As stated above, LPS did not activate Weibel-Palade body exocytosis (Fig. 1D). However, LPS potently activated induction of MyD88-dependent IL-8 production in HAECs after stimulation for 4 h (Fig. 3A). Thus, the results shown in Figs. 1D and 3A suggest that endothelial TLR4 lacks the ability to induce rapid Weibel-Palade body exocytosis without *de novo* protein synthesis. Similarly to LPS, PGN did not activate Weibel-Palade body exocytosis (Fig. 1D). Also, PGN did not induce IL-8 production after stimulation for 4 h in HAECs, whereas LTA did (Fig. 3A). However, our preparation of PGN had activities to induce TNF-α production in THP-1 monocytes (Fig. 3B) and TLR- and MyD88-dependent activation of NF-κB in HEK293 cells (Fig. 3C) in a way similar to that in the case of other TLR2 agonists. These results suggest that HAECs lack the ability to respond to PGN.

Induction of Weibel-Palade Body Exocytosis through TLR2—We then focused on LTA- and bacterial lipopeptide-induced Weibel-Palade body exocytosis. It has been reported that LTA and bacterial lipopeptides are TLR2 agonists (Table 1). In HUVECs, the lipopeptide FSL-1 induced VWF release (Fig. 4A). We found that this response was enhanced by increased expression of TLR2 by gene transfection (Fig. 4A). This result suggests that TLR2 recognition of bacterial constituents directly activates Weibel-Palade body exocytosis. Moreover, transfection of mutated TLR2 (P681H), which lacks the ability to interact with MyD88 (26), suppressed the release (Fig. 4B), consistent with the results presented in Figs. 1D and 2A showing that MyD88 was involved in the induction of Weibel-Palade exocytosis. In HAECs, knockdown of TLR2 expression resulted in almost complete suppression of VWF release by Pam_3CSK_4, FSL-1, MALP-2, and LTA (Fig. 4B). Moreover, knockdown of TLR6 expression resulted in a decrease in the activities of LTA, FSL-1, and MALP-2 and even that of Pam_3CSK_4 (Fig. 4B). In contrast to this, TLR1 interference did not affect VWF release (Fig. 4B), consistent with our observation that HAECs express very low levels of TLR1 mRNA compared with the levels of TLR2 mRNA (data not shown). These results suggest that endothelial recognition of pathogens by TLR2, or to a lesser extent by TLR6, contributes to induction of Weibel-Palade body exocytosis.
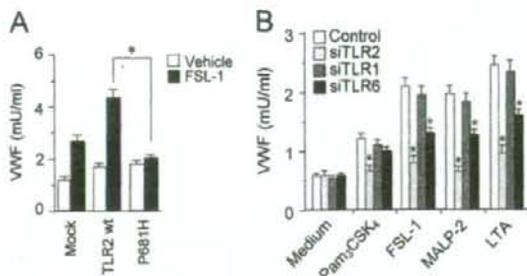
Involvement of PLCγ Activation in Weibel-Palade Body Exocytosis—Recent studies have shown that TLR2 signal transduction results in an increase of intracellular calcium level (27, 28). Indeed, we found that the intracellular calcium chelator BAPTA-AM suppressed LTA-induced exocytosis (Fig. 5A). We

TABLE 1
Bacterial cell wall constituents used in this study

Substance	Origin (Ref.)	TLR recognition in human cells (Ref.)
LTA	*S. aureus*	TLR2 (7)
LPS	*E. coli*	TLR4 (10)
LPS	*S. minnesota*	TLR4 (10)
Flagellin	*S. typhimurium*	TLR5 (9)
PGN	*S. aureus*	TLR2 (8)
Pam_3CSK_4	Synthesis (*E. coli*) (16)	TLR1/TLR2 (41)
FSL-1	Synthesis (*M. salivarium*) (18)	TLR2/TLR6 (17)
MALP-2	Synthesis (*M. fermentans*) (19)	TLR2/TLR6 (55)
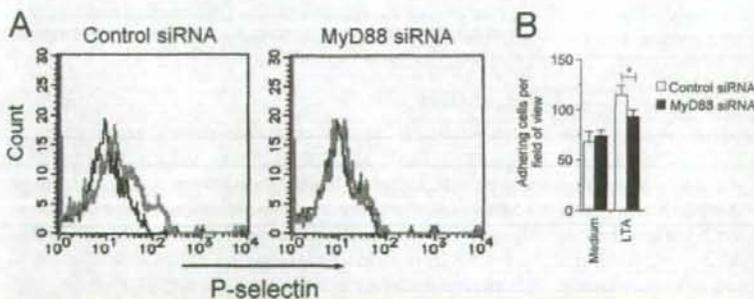
FIGURE 2. **MyD88-dependent P-selectin externalization by LTA.** *A*, HAECs transfected with MyD88-specific or control siRNA were stimulated with 10 µg/ml LTA for 60 min, and then surface P-selectin was detected by flow cytometry. *Shaded histogram*, not stimulated; *gray*, stimulated with LTA. *B*, HAECs transfected with MyD88-specific or control siRNA were stimulated with 10 µg/ml LTA for 60 min, and monocytes stained with conA-Alexa594 were then allowed to adhere for 20 min. Adhesion of red fluorescent cells was quantified in three fields per well by using an image analysis system. Each value is the mean ± S.D. ($n = 3$). *, $p < 0.01$.

– 397 –

FIGURE 3. **Stimulatory activities of LPS and PGN in HAECs.** *A*, HAECs transfected with MyD88-specific or control siRNA were stimulated with LTA (0.1–10 μg/ml), PGN (0.1–10 μg/ml), and LPS (1–100 ng/ml) for 4 h, and then the amounts of IL-8 released into the media were measured. Each value is the mean ± S.D. (*n* = 3). *B*, THP-1 cells were stimulated with PGN (0.1–10 μg/ml), LTA (0.1–10 μg/ml), and FSL-1 (10–1 μg/ml) for 6 h, and then the amounts of TNF-α released into the media were measured. Each value is the mean ± S.D. (*n* = 3). *C*, HEK293 cells stably expressing TLR2, and control cells were prepared and then transfected with MyD88-specific siRNA and NF-κB-driven luciferase gene. The cells were stimulated with Pam₃CSK₄ (0.1–10 μg/ml), FSL-1 (0.01–1 μg/ml), MALP-2 (0.01–1 μg/ml), LTA (0.1–10 μg/ml), PGN (0.1–10 μg/ml), and LPS (1–100 ng/ml) for 6 h, and then luciferase activity was measured. Each value is the mean ± S.D. (*n* = 3).

FIGURE 4. **Involvement of TLR2 in Weibel-Palade body exocytosis.** *A*, HUVECs transfected with WT or P681H mutant of TLR2 or with a control plasmid were stimulated with 1 μg/ml FSL-1 for 60 min, and then the amounts of VWF released into the media were measured. Each value is the mean ± S.D. (*n* = 3). *B*, HAECs transfected with TLR1-, TLR2-, or TLR6-specific or control siRNA were stimulated with Pam₃CSK₄ (10 μg/ml), FSL-1 (1 μg/ml), MALP-2 (1 μg/ml), and LTA (10 μg/ml) for 60 min, and then the amounts of VWF released into the media were measured. Each value is the mean ± S.D. (*n* = 3). *, *p* < 0.05.

therefore examined the role of PLCγ, a common regulator of intracellular calcium release by generating inositol 1,4,5-triphosphate (29), during TLR2-mediated Weibel-Palade body exocytosis. We found that the PLCγ inhibitor U-73122 significantly suppressed TLR2 agonist-induced VWF release (Fig. 5*B*). Because PLCγ isoforms are thought to be activated by phosphatidylinositol 3,4,5-trisphosphate, the product of phosphatidylinositol 3-kinases (PI3Ks) (29), TLR2-mediated exocytosis was suppressed by the chemical inhibitor of PI3K LY294002 (data not shown). However, downstream of TLR/IL-1R, activation of PI3K is regulated through a MyD88-independent machinery (30), conflicting with our results showing that Weibel-Palade body exocytosis requires MyD88 (Figs. 1*D* and 2*A*). Because enzymatic activity of PLCγ is also regulated by tyrosine phosphorylation (31), we tested whether this event was mediated by MyD88. Phosphorylation of PLCγ1 at the Tyr-738 residue was induced by LTA stimulation (Fig. 5*C*). Interestingly, this activity was efficiently suppressed by knockdown of MyD88 expression but not by knockdown of IRAK-1 expression (Fig. 5*C*). MyD88-dependent activation of PLCγ was also observed in TLR2-overexpressed 293 cells used as non-endothelial cells (data not shown). These results suggest that TLR2-mediated rapid Weibel-Palade body exocytosis is regulated by

activation of PLCγ through MyD88-dependent tyrosine phosphorylation.

We also investigated the role of PLCγ in TLR2-mediated NF-κB signaling. U-73122 treatment clearly suppressed TLR2 agonist-induced production of the NF-κB-driven chemokine IL-8 in HAECs (Fig. 5*D*). U-73122 treatment also suppressed LTA-induced phosphorylation and degradation of IκBα in HAECs (Fig. 5*E*). These results suggest that the MyD88-PLCγ pathway also mediates inflammatory responses through NF-κB activation in endothelial cells.

Regulation of TLR2-mediated Weibel-Palade Body Exocytosis—The results shown in Fig. 4 (*A* and *B*) raised the possibility that alteration of endothelial TLR2 expression affects the magnitude of Weibel-Palade body exocytosis. We examined TLR2-mediated exocytosis in the presence of vascular modulators, IFN-γ or laminar flow, which are known to affect TLR2 expression in endothelial cells of human origin. Consistent with the results of a previous study (32), treatment with IFN-γ increased TLR2 expression level in HAECs (Fig. 6*A*). Under this condition, the magnitude of TLR2-mediated exocytosis was significantly increased (Fig. 6*B*). In contrast to this, TLR2 expression slightly decreased in HAECs incubated under laminar flow (Fig. 6*C*), consistent with the results of a previous study (33). We found that laminar flow decreased the magnitude of TLR2-mediated exocytosis (Fig. 6*D*).

DISCUSSION

The major finding of this study is that aortic endothelial cells respond to several bacterial constituents that stimulate TLR2, leading to induction of Weibel-Palade body exocytosis through a MyD88-dependent mechanism without *de novo* protein synthesis. During this process, release of VWF and externalization of P-selectin were induced, by which rolling and adhesion of platelets and leukocytes and thrombus formation in the local vessel walls may be promoted (34, 35). The pathological role of this phenomenon *in vivo* may be support by the observations in mouse experiments, *i.e.* slight increases of local leukocyte-endothelial interaction after LTA administration (36) and soluble P-selectin level in serum after administration of the synthetic
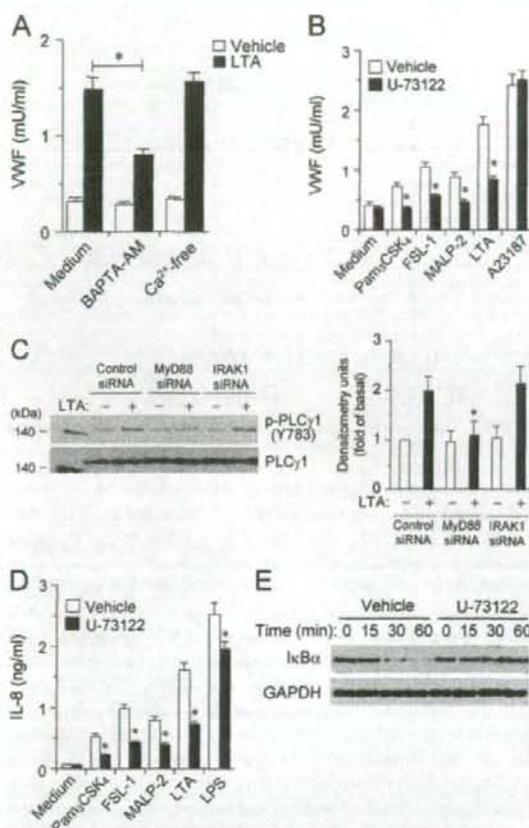
FIGURE 5. **PLC γ-mediation of TLR2-activated Weibel-Palade body exocytosis and NF-κB activation.** *A,* confluent HAECs were pretreated with 20 μM BAPTA-AM for 30 min or incubated in Ca^{2+}-free media. Then the cells were washed and stimulated with 10 μg/ml LTA for 60 min in Ca^{2+}-free media. The amounts of VWF released into the media were measured by ELISA. Each value is the mean ± S.D. ($n = 3$). *, $p < 0.01$. *B,* HAECs were pretreated with 10 μM U-73122 for 30 min and then washed and stimulated with Pam$_3$CSK$_4$ (10 μg/ml), FSL-1 (1 μg/ml), MALP-2 (1 μg/ml), LTA (10 μg/ml), and A23187 (1 μM) for 60 min. The amounts of VWF released into the media were measured by ELISA. Each value is the mean ± S.D. ($n = 3$). *, *versus* vehicle group, $p < 0.01$. *C,* HAECs transfected with MyD88- or IRAK1-specific or control siRNA were stimulated with 10 μg/ml LTA for 90 min. Immunoblot analysis was then performed to examine the expression of phosphorylated PLCγ1 (Y783) and total PLCγ1 (*left*). Immunoreactive bands were quantified by a densitometer (*right*). Results are expressed as means ± S.D. of three independent experiments. *, *versus* control group, $p < 0.01$. *D,* HAECs were pretreated with 10 μM U73122 for 30 min and then washed and stimulated with Pam$_3$CSK$_4$ (10 μg/ml), FSL-1 (1 μg/ml), MALP-2 (1 μg/ml), LTA (10 μg/ml), and A23187 (1 μM) for 4 h. The amounts of IL-8 released into the media were measured by ELISA. Each value is the mean ± S.D. ($n = 3$). *, *versus* vehicle group, $p < 0.01$. *E,* HAECs were pretreated with 10 μM U73122 for 30 min and then washed and stimulated with 10 μg/ml LTA for the indicated period. Immunoblot analysis was then performed to examine the expression of IκBα and glyceraldehyde-3-phosphate dehydrogenase (*GAPDH*).

lipopeptide FSL-1.[3] Sequentially or simultaneously, both PLCγ- and IRAK1-mediated signaling pathways activate NF-κB, by which production of various proinflammatory cyto-

---

[3] T. Into, Y. Kanno, J.-i. Dohkan, M. Nakashima, M. Inomata, K.-i. Shibata, C. J. Lowenstein, and K. Katsushita, unpublished data.
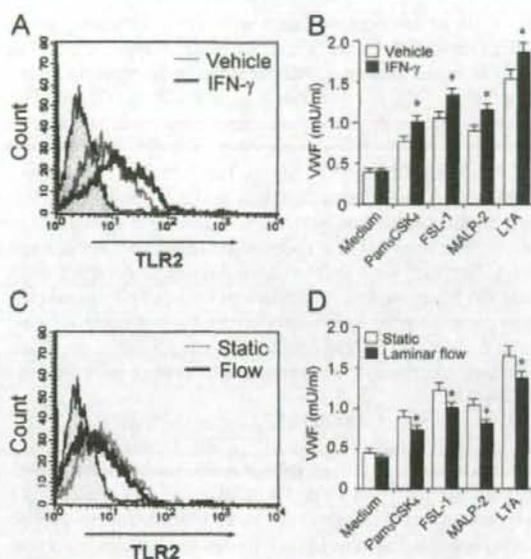
FIGURE 6. **Regulation of TLR2-mediated Weibel-Palade body exocytosis.** *A* and *B,* HAECs were treated with IFN-γ for 12 h. Surface TLR2 expression was detected by flow cytometry (*A*). The *shaded histogram* indicates cells stained with control antibody. The cells were washed and stimulated with Pam$_3$CSK$_4$ (10 μg/ml), FSL-1 (1 μg/ml), MALP-2 (1 μg/ml), and LTA (10 μg/ml) for 60 min. The amounts of VWF released into the media were measured by ELISA (*B*). Each value is the mean ± S.D. ($n = 3$). *, *versus* vehicle group, $p < 0.05$. *C* and *D,* HAECs were incubated under laminar flow for 12 h. Surface TLR2 expression was detected by flow cytometry (*C*). The *shaded histogram* indicates cells stained with control antibody. The cells were then stimulated with Pam$_3$CSK$_4$ (10 μg/ml), FSL-1 (1 μg/ml), MALP-2 (1 μg/ml), and LTA (10 μg/ml) for 60 min. The amounts of VWF released into the media were measured by ELISA (*D*). Each value is the mean ± S.D. ($n = 3$). *, *versus* static group, $p < 0.05$.

kines, and expression of adhesion molecules such as ICAM-1 are induced to promote adherence and activation of platelets and leukocytes (37). The delayed Weibel-Palade body exocytosis with *de novo* protein synthesis is further activated in the cells. Therefore, endothelial TLR2 may be able to function as a primary initiator and a modulator of artery inflammation through these early-phase endothelial responses after recognition of cognate agonists.

We investigated the responsiveness of HAECs toward common bacterial constituents. For the TLR2 agonists, we prepared several compounds that have already been proposed to function as TLR2 agonists, because TLR2 forms a complicated recognition system and because human endothelial cells from different vascular beds show different degrees of responsiveness to TLR2 agonists (32, 38, 39). Unexpectedly, PGN, unlike other TLR2 agonists, could not activate either Weibel-Palade body exocytosis or IL-8 production (Figs. 1*D* and 3*A*). The issue of recognition of PGN by TLR2 is still controversial. The existence of an intracellular receptor for PGN (NOD2) further complicates this matter. However, Gupta's group recently concluded that PGN is in fact recognized by TLR2 by showing that muramidase treatment of PGN abolished the TLR2-stimulating activity (8). We showed that recognition of our PGN was at least dependent on TLR2 (Fig. 3*A*). It has been shown that PGN directly binds TLR2 *per se* (40), whereas bacterial lipopeptides

are thought to directly interact with TLR2-associated molecules such as CD14 and LBP but not with TLR2 *per se* (7, 41, 42), suggesting the existence of different ligand-recognition mechanisms by TLR2. Furthermore, a novel family of PGN-binding proteins such as peptidoglycan recognition proteins has been found (43) and might enable discrimination of PGN from other TLR2 agonists. Thus, PGN may be recognized by a TLR2 recognition system different from that for LTA and lipoproteins/lipopeptides. Collectively, HAECs express functional TLR2 to respond to several TLR2 agonists, including lipopeptides and LTA, but may lack a PGN-recognition system resulting in an inability to respond to PGN. Moreover, aortic endothelial cells may particularly recognize diacylglyceride-containing bacterial lipid derivatives (LTA and bacterial lipopeptides), recognition of which has recently been reported to depend on TLR6 and CD36 (11).

We also showed that the TLR4 agonist LPS did not activate Weibel-Palade body exocytosis (Fig. 1D). Although the reason for this is not clear, several lines of evidence obtained in previous studies may provide an explanation. For example, TLR4 expression has been reported to localize intracellularly in artery endothelial cells (44). This observation suggests that TLR4 in artery endothelial cells may be lacking in induction of phospholipid-dependent signaling events, including PLCγ activation, which are commonly intrinsic to the signaling receptors spanning the cell membrane. Further investigation is needed to determine the reason.

Several properties of endothelial TLR2 have been proposed to be involved in the development of atherosclerosis. First, endothelial TLR2 expression is enhanced by proinflammatory stimuli, such as TNF-α, IFN-γ, and LPS (32), and by SP-1-dependent machinery in areas of disturbed blood flow such as lesion predilection within the aortic tree and heart (33). The expression level of TLR2 is indeed increased in an atherosclerotic lesion in humans (45). Furthermore, a recent study has revealed that complete deficiency of TLR2 in atherosclerosis-prone LDLR-null mice leads to an apparent reduction in the formation of lesions (46). Proinflammatory signaling pathways downstream of TLR2 have been thought to be activated through TIRAP/Mal, MyD88, IRAK-1, and TRAF6 in endothelial cells. Other pathways involving PI3K and the downstream protein kinase Akt/PKB (47), the Rho family GTPase Rac1 (48), and the redox-activated mitogen-activated protein kinase kinase kinase ASK1 (49) also link TLR2 signaling to the NF-κB pathway. In this study, we showed that PLCγ also mediated the NF-κB pathway downstream of TLR2 in HAECs, although involvement of PLCγ in the TLR2 proinflammatory signaling has been described in several reports (27, 50). Because PLCγ isoforms are thought to be activated by both generation of phosphatidylinositol 3,4,5-triphosphate by PI3K and tyrosine phosphorylation, we found the latter process downstream of TLR2 was dependent on MyD88 but not IRAK-1 (Fig. 5C). Recent studies have suggested a linkage of TLRs and tyrosine kinases, including Syk via MyD88-STAP-2 interaction (51) and Btk via direct interaction with TIR domain (52), both of which have been shown to activate PLCγ isoforms. Moreover, Btk-induced phosphorylation of TIRAP/Mal has recently been reported to play an important role in TLR signal transduction
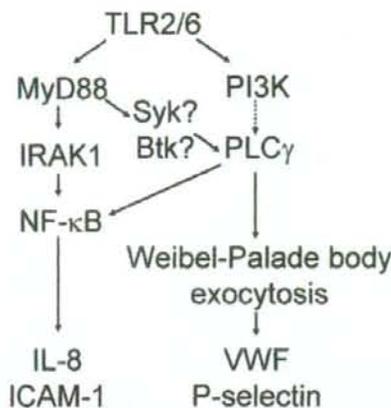

FIGURE 7. **The proposed schematic for TLR2 regulation of early-phase inflammatory signaling in human aortic endothelial cells.**

(53), which may occur at a phosphatidylinositol diphosphate-rich membrane compartment after recruitment of MyD88 to membrane-localized TIRAP/Mal (54). A schematic of signaling pathways proposed here is shown in Fig. 7.

Endothelial activation by several proinflammatory agents has been shown to increase endothelial responsiveness toward TLR2 agonists via up-regulation of TLR2 expression (32). Increased endothelial TLR2 expression increased the magnitude of TLR2-mediated exocytosis of Weibel-Palade bodies (Fig. 6B) and endothelial responses (38), suggesting enhanced responsiveness of endothelial cells to pathogens in inflamed lesions. In contrast, fluid shear decreased the magnitude of TLR2 ligand-stimulated Weibel-Palade body exocytosis (Fig. 6D). Physiological fluid shear stress has been suggested to have atheroprotective effects *in vivo*, because atherosclerosis preferentially occurs in an area of disturbed flow or a low level of shear stress, whereas regions with steady laminar flow and physiological shear stress are protected. Disturbed flow or a low level of shear stress has been reported to regulate expression of various regulatory molecules of endothelial activation, by which atherosclerotic processes may be accelerated in the sites. These observations are consistent with the previous finding that physiological fluid shear stress decreases endothelial TLR2 expression via impaired activity of the transcriptional factor SP1 (33). Thus, our results raise the possibility that bacterial constituent-induced Weibel-Palade body exocytosis can be physiologically or pathologically regulated in particular circumstances of the vessel wall.

In conclusion, our study focused on endothelial exocytosis induced by bacterial pathogens and showed a linkage between endothelial innate recognition of pathogens and early-phase endothelial inflammatory responses. Our results may provide a new insight into the role of endothelial TLR2 in the initiation and modulation of vascular inflammation or atherogenic responses.

REFERENCES

1. Lowenstein, C. J., Morrell, C. N., and Yamakuchi, M. (2005) *Trends Cardiovasc. Med.* **15**, 302–308
2. Rondaij, M. G., Bierings, R., Kragt, A., van Mourik, J. A., and Voorberg, J.

– 400 –

(2006) *Arterioscler. Thromb. Vasc. Biol.* **26**, 1002–1007

3. Danesh, J. (1999) *Am. Heart J.* **138**, S434–S437
4. Desvarieux, M., Demmer, R. T., Rundek, T., Boden-Albala, B., Jacobs, D. R., Jr., Sacco, R. L., and Papapanou, P. N. (2005) *Circulation* **111**, 576–582
5. Akira, S., and Takeda, K. (2004) *Nat. Rev. Immunol.* **4**, 499–511
6. Kirschning, C. J., and Schumann, R. R. (2002) *Curr. Top. Microbiol. Immunol.* **270**, 121–144
7. Schroder, N. W., Morath, S., Alexander, C., Hamann, L., Hartung, T., Zahringer, U., Gobel, U. B., Weber, J. R., and Schumann, R. R. (2003) *J. Biol. Chem.* **278**, 15587–15594
8. Dziarski, R., and Gupta, D. (2005) *Infect. Immun.* **73**, 5212–5216
9. Reed, K. A., Hobert, M. E., Kolenda, C. E., Sands, K. A., Rathman, M., O'Connor, M., Lyons, S., Gewirtz, A. T., Sansonetti, P. J., and Madara, J. L. (2002) *J. Biol. Chem.* **277**, 13346–13353
10. Tapping, R. I., Akashi, S., Miyake, K., Godowski, P. J., and Tobias, P. S. (2000) *J. Immunol.* **165**, 5780–5787
11. Hoebe, K., Georgel, P., Rutschmann, S., Du, X., Mudd, S., Crozat, K., Sovath, S., Shamel, L., Hartung, T., Zahringer, U., and Beutler, B. (2005) *Nature* **433**, 523–527
12. Jeannin, P., Bottazzi, B., Sironi, M., Doni, A., Rusnati, M., Presta, M., Maina, V., Magistrelli, G., Haeuw, J. F., Hoeffel, G., Thieblemont, N., Corvaia, N., Garlanda, C., Delneste, Y., and Mantovani, A. (2005) *Immunity* **22**, 551–560
13. Mullally, S. C., and Kubes, P. (2004) *Circ. Res.* **95**, 657–659
14. Tobias, P., and Curtiss, L. K. (2005) *J. Lipid Res.* **46**, 404–411
15. Michelsen, K. S., Doherty, T. M., Shah, P. K., and Arditi, M. (2004) *J. Immunol.* **173**, 5901–5907
16. Hoffmann, P., Heinle, S., Schade, U. F., Loppnow, H., Ulmer, A. J., Flad, H. D., Jung, G., and Bessler, W. G. (1988) *Immunobiology* **177**, 158–170
17. Fujita, M., Into, T., Yasuda, M., Okusawa, T., Hamahira, S., Kuroki, Y., Eto, A., Nisizawa, T., Morita, M., and Shibata, K. (2003) *J. Immunol.* **171**, 3675–3683
18. Shibata, K., Hasebe, A., Into, T., Yamada, M., and Watanabe, T. (2000) *J. Immunol.* **165**, 6538–6544
19. Muhlradt, P. F., Kiess, M., Meyer, H., Sussmuth, R., and Jung, G. (1997) *J. Exp. Med.* **185**, 1951–1958
20. Into, T., Kiura, K., Yasuda, M., Kataoka, H., Inoue, N., Hasebe, A., Takeda, K., Akira, S., and Shibata, K. (2004) *Cell Microbiol.* **6**, 187–199
21. Matsushita, K., Morrell, C. N., Cambien, B., Yang, S. X., Yamakuchi, M., Bao, C., Hara, M. R., Quick, R. A., Cao, W., O'Rourke, B., Lowenstein, J. M., Pevsner, J., Wagner, D. D., and Lowenstein, C. J. (2003) *Cell* **115**, 139–150
22. Dimmeler, S., Haendeler, J., Rippmann, V., Nehls, M., and Zeiher, A. M. (1996) *FEBS Lett.* **399**, 71–74
23. Doran, K. S., Engelson, E. J., Khosravi, A., Maisey, H. C., Fedtke, I., Equils, O., Michelsen, K. S., Arditi, M., Peschel, A., and Nizet, V. (2005) *J. Clin. Invest.* **115**, 2499–2507
24. Bermpohl, D., Halle, A., Freyer, D., Dagand, E., Braun, J. S., Bechmann, I., Schroder, N. W., and Weber, J. R. (2005) *J. Clin. Invest.* **115**, 1607–1615
25. Talreja, J., Kabir, M. H., Filla, M. B., Stechschulte, D. J., and Dileepan, K. N. (2004) *Immunology* **113**, 224–233
26. Xu, Y., Tao, X., Shen, B., Horng, T., Medzhitov, R., Manley, J. L., and Tong, L. (2000) *Nature* **408**, 111–115
27. Chun, J., and Prince, A. (2006) *J. Immunol.* **177**, 1330–1337
28. Supajatura, V., Ushio, H., Nakao, A., Akira, S., Okumura, K., Ra, C., and Ogawa, H. (2002) *J. Clin. Invest.* **109**, 1351–1359
29. Bae, Y. S., Cantley, L. G., Chen, C. S., Kim, S. R., Kwon, K. S., and Rhee, S. G.

30. Davis, C. N., Mann, E., Behrens, M. M., Gaidarova, S., Rebek, M., Rebek, J., Jr., and Bartfai, T. (2006) *Proc. Natl. Acad. Sci. U. S. A.* **103**, 2953–2958
31. Law, C. L., Chandran, K. A., Sidorenko, S. P., and Clark, E. A. (1996) *Mol. Cell Biol.* **16**, 1305–1315
32. Faure, E., Thomas, L., Xu, H., Medvedev, A., Equils, O., and Arditi, M. (2001) *J. Immunol.* **166**, 2018–2024
33. Dunzendorfer, S., Lee, H. K., and Tobias, P. S. (2004) *Circ. Res.* **95**, 684–691
34. Andre, P., Denis, C. V., Ware, J., Saffaripour, S., Hynes, R. O., Ruggeri, Z. M., and Wagner, D. D. (2000) *Blood* **96**, 3322–3328
35. Massberg, S., Brand, K., Gruner, S., Page, S., Muller, E., Muller, I., Bergmeier, W., Richter, T., Lorenz, M., Konrad, I., Nieswandt, B., and Gawaz, M. (2002) *J. Exp. Med.* **196**, 887–896
36. Yipp, B. G., Andonegui, G., Howlett, C. J., Robbins, S. M., Hartung, T., Ho, M., and Kubes, P. (2002) *J. Immunol.* **168**, 4650–4658
37. Collins, T., Read, M. A., Neish, A. S., Whitley, M. Z., Thanos, D., and Maniatis, T. (1995) *FASEB J.* **9**, 899–909
38. Bulut, Y., Faure, E., Thomas, L., Equils, O., and Arditi, M. (2001) *J. Immunol.* **167**, 987–994
39. Faure, E., Equils, O., Sieling, P. A., Thomas, L., Zhang, F. X., Kirschning, C. J., Polentarutti, N., Muzio, M., and Arditi, M. (2000) *J. Biol. Chem.* **275**, 11058–11063
40. Iwaki, D., Mitsuzawa, H., Murakami, S., Sano, H., Konishi, M., Akino, T., and Kuroki, Y. (2002) *J. Biol. Chem.* **277**, 24315–24320
41. Manukyan, M., Triantafilou, K., Triantafilou, M., Mackie, A., Nilsen, N., Espevik, T., Wiesmuller, K. H., Ulmer, A. J., and Heine, H. (2005) *Eur. J. Immunol.* **35**, 911–921
42. Schroder, N. W., Heine, H., Alexander, C., Manukyan, M., Eckert, J., Hamann, L., Gobel, U. B., and Schumann, R. R. (2004) *J. Immunol.* **173**, 2683–2691
43. Dziarski, R., and Gupta, D. (2006) *Cell Microbiol.* **8**, 1059–1069
44. Dunzendorfer, S., Lee, H. K., Soldau, K., and Tobias, P. S. (2004) *FASEB J.* **18**, 1117–1119
45. Edfeldt, K., Swedenborg, J., Hansson, G. K., and Yan, Z. Q. (2002) *Circulation* **105**, 1158–1161
46. Mullick, A. E., Tobias, P. S., and Curtiss, L. K. (2005) *J. Clin. Invest.* **115**, 3149–3156
47. Martin, M., Schifferle, R. E., Cuesta, N., Vogel, S. N., Katz, J., and Michalek, S. M. (2003) *J. Immunol.* **171**, 717–725
48. Arbibe, L., Mira, J. P., Teusch, N., Kline, L., Guha, M., Mackman, N., Godowski, P. J., Ulevitch, R. J., and Knaus, U. G. (2000) *Nat. Immunol.* **1**, 533–540
49. Into, T., and Shibata, K. (2005) *Cell Microbiol.* **7**, 1305–1317
50. Lee, C. W., Chien, C. S., and Yang, C. M. (2004) *Am. J. Physiol.* **286**, L921–L930
51. Sekine, Y., Yumioka, T., Yamamoto, T., Muromoto, R., Imoto, S., Sugiyma, K., Oritani, K., Shimoda, K., Minoguchi, M., Akira, S., Yoshimura, A., and Matsuda, T. (2006) *J. Immunol.* **176**, 380–389
52. Horwood, N. J., Page, T. H., McDaid, J. P., Palmer, C. D., Campbell, J., Mahon, T., Brennan, F. M., Webster, D., and Foxwell, B. M. (2006) *J. Immunol.* **176**, 3635–3641
53. Gray, P., Dunne, A., Brikos, C., Jefferies, C. A., Doyle, S. L., and O'Neill, L. A. (2006) *J. Biol. Chem.* **281**, 10489–10495
54. Kagan, J. C., and Medzhitov, R. (2006) *Cell* **125**, 943–955
55. Nakao, Y., Funami, K., Kikkawa, S., Taniguchi, M., Nishiguchi, M., Fukumori, Y., Seya, T., and Matsumoto, M. (2005) *J. Immunol.* **174**, 1566–1573

(1998) *J. Biol. Chem.* **273**, 4465–4469

STEM CELLS

TISSUE-SPECIFIC STEM CELLS

A Novel Stem Cell Source for Vasculogenesis in Ischemia: Subfraction of Side Population Cells from Dental Pulp

KOICHIRO IOHARA,[a] LI ZHENG,[a] HIROAKI WAKE,[b] MASATAKA ITO,[c] JUNICHI NABEKURA,[b] HIDEAKI WAKITA,[d] HIROSHI NAKAMURA,[e] TAKESHI INTO,[a] KENJI MATSUSHITA,[a] MISAKO NAKASHIMA[a]

[a]Department of Oral Disease Research, National Institute for Longevity Sciences, National Center for Geriatrics and Gerontology, Obu, Aichi, Japan; [b]Department of Developmental Physiology, National Institute for Physiological Sciences, Okazaki, Aichi, Japan; [c]Department of Developmental Anatomy and Regenerative Medicine, National Defense Medical College, Tokorozawa, Saitama, Japan; [d]Department of Vascular Dementia Research, National Institute for Longevity Sciences, National Center for Geriatrics and Gerontology, Obu, Aichi, Japan; [e]Department of Endodontics, School of Dentistry, Aichigakuin University, Nagoya, Aichi, Japan

ABSTRACT

Cell therapy with stem cells and endothelial progenitor cells (EPCs) to stimulate vasculogenesis as a potential treatment for ischemic disease is an exciting area of research in regenerative medicine. EPCs are present in bone marrow, peripheral blood, and adipose tissue. Autologous EPCs, however, are obtained by invasive biopsy, a potentially painful procedure. An alternative approach is proposed in this investigation. Permanent and deciduous pulp tissue is easily available from teeth after extraction without ethical issues and has potential for clinical use. We isolated a highly vasculogenic subfraction of side population (SP) cells based on CD31 and CD146, from dental pulp. The CD31⁻;CD146⁻ SP cells, demonstrating CD34⁺ and vascular endothelial growth factor-2 (VEGFR2)/Flk1⁺, were similar to EPCs. These cells were distinct from the hematopoietic lineage as *CD11b, CD14,* and *CD45* mRNA were not expressed. They showed high proliferation and migration activities and multilineage differentiation potential including vasculogenic potential. In models of mouse hind limb ischemia, local transplantation of this subfraction of SP cells resulted in successful engraftment and an increase in the blood flow including high density of capillary formation. The transplanted cells were in proximity of the newly formed vasculature and expressed several proangiogenic factors, such as *VEGF-A, G-CSF, GM-CSF,* and *MMP3.* Conditioned medium from this subfraction showed mitogenic and antiapoptotic activity on human umbilical vein endothelial cells. In conclusion, subfraction of SP cells from dental pulp is a new stem cell source for cell-based therapy to stimulate angiogenesis/vasculogenesis during tissue regeneration. STEM CELLS 2008;26: 2408–2418

Disclosure of potential conflicts of interest is found at the end of this article.

INTRODUCTION

The potential application of stem/progenitor cells to treat ischemia has generated genuine excitement in regenerative medicine [1, 2]. Endothelial progenitor cells (EPCs) are of utility to achieve corrective vasculogenesis to treat cardiac, cerebral, and limb ischemia. The characteristic features of EPCs are CD34-, CD133-, and vascular endothelial growth factor-2 (VEGFR2)-positive cells [3–5]. In both embryonic and adult human aorta CD34⁺;CD31⁻ cells differentiate into endothelial cells [6, 7]. Human adipose tissue-derived stromal-vascular fraction contains CD34⁺;CD31⁻ cells with potential to differentiate into endothelial cells [8].

The human dental pulp is a highly vascular tissue that is enriched in stem/progenitor cells [9–11]. The ready availability of dental pulp from teeth obtained during orthodontic treatment and extracted third molars circumvents any ethical concerns and is a definite advantage. In addition, their immunosuppressive properties [10] may be useful for allogeneic transplantation. Recent work in our laboratory identified stem/progenitor cells in porcine dental pulp by the use of fluorescent Hoechst dye 33342 to isolate side population (SP) cells [12]. The subfractionation of SP cells that were CD34⁺;VEGFR2/Flk1⁺ into CD31⁻;CD146⁻ and CD31⁺;CD146⁻ cells revealed distinct properties, the former dif-

ferentiated into endothelial cells in vitro. In addition, the CD31⁻;CD146⁻ SP cell subfraction caused functional revascularization of hind limb ischemia in vivo and is the topic of this investigation.

MATERIALS AND METHODS

Isolation by Flow Cytometry

The primary pulp cells from porcine tooth germ were separated and labeled with Hoechst 33342 (Sigma, St. Louis, http://www.sigmaaldrich.com) as previously described [12]. Then the cells were preincubated with mouse BD Fc Block (BD Biosciences, San Jose, CA, http://www.bdbiosciences.com) for 30 minutes at 4°C to reduce nonspecific binding. The cells were further incubated with the mouse IgG1 negative control (MCA928) (AbD Serotec Ltd., Oxford, U.K., http://www.serotec.com), mouse IgG1 negative control (phycoerythrin [PE]) (MCA928PE) (AbD Serotec Ltd.), mouse IgG1 negative control (fluorescein isothiocyanate [FITC]) (MCA928FITC) (AbD Serotec Ltd.), mouse anti-porcine CD31 (PE) (LCI-4) (AbD Serotec Ltd.), and mouse anti-human CD146 (FITC) (OJ79c) (AbD Serotec Ltd.) in phosphate-buffered saline (PBS) with 20% fetal bovine serum (Invitrogen Corp., Carlsbad, CA, http://www.invitrogen.com) for 60 minutes at 4°C. Those were resuspended in HEPES buffer containing 2 μg/ml propidium iodide (Sigma). Analysis/sorting of cells was performed using a flow cytometer JSAN (Bay Bioscience, Kobe, Japan, http://www.baybio.co.jp).

Cell Cultures

We investigated the most suitable supplement of culture medium, EBM2 (Cambrex Bio Science Walkersville, Inc., Walkersville, MD, http://www.cambrex.com), including growth factors such as basic fibroblast growth factor (bFGF), insulin-like growth factor I (IGF1), epidermal growth factor (EGF), and vascular endothelial growth factor-A (VEGF-A) (Cambrex Bio Science, Inc.). The optimal concentration of porcine serum (JRH Biosciences, Inc., Lenexa, KS, http://www.jrhbio.com) was also determined to maintain all the sorted cells, CD31⁻;CD146⁻ SP cells, CD31⁺;CD146⁻ SP cells, and CD31⁺;CD146⁺ SP cells. Each cell fraction was plated into 35-mm collagen type I-coated dishes (Asahi Technoglass Corp., Funabashi, Japan, http://www.atgc.co.jp) in EBM2 supplemented with suitable growth factors. Medium was changed every 4–5 days. Once cells reached 50%–60% confluence, they were detached by incubation with 0.02% EDTA at 37°C for 10 minutes and subcultured at a 1:4 dilution under the same conditions for more than 20 passages.

Expression of Cell Surface Markers

To characterize the phenotype of the CD31⁻ SP cells and CD31⁺ SP cells, the freshly isolated cells were double-stained with each antibody against CD146 (FITC) (OJ79c) (AbD Serotec Ltd.), CD11b (biotin) (M1/70) (BD Biosciences), CD14 (Alexa Flour 647) (TuK4) (AbD Serotec Ltd.), CD90 (Alexa Flour 647) (F15–42-1) (AbD Serotec Ltd.), CD117/c-kit (allophycocyanin [APC]) (A3C6E2) (Miltenyi Biotec, Bergisch Gladbach, Germany, http://www.miltenyibiotec.com), CD150 (FITC) (A12) (AbD Serotec Ltd.), CD271 (APC) (ME20.4–1H4) (Miltenyi Biotec) together with CD31 antibody after Hoechst 33342 labeling, and analyzed by flow cytometry. Streptavidin (PE-Cy7) (eBioscience, San Diego, http://www.ebioscience.com) was used for a secondary antibody of CD11b. In case of CD34 and VEGFR2/Flk1, the isolated CD31⁻ SP cells and CD31⁺ SP cells were cultured for 5 days to remove the CD31 antibody bound on the cell surface, and the expanded secondary cells were immunolabeled with antibodies against CD34 (QBEnd-10) (Immunotech, Cedex, France, http://www.beckmancoulter.com/products/pr_immunology.asp) and VEGFR2/Flk1 (30457) (Upstate, Spartanburg, SC, http://www.upstate.com), respectively, and goat anti-rabbit IgG (Alexa 488) (Molecular Probes, Eugene, OR, http://probes.invitrogen.com) as the secondary antibody.

Real-Time Reverse Transcription-Polymerase Chain Reaction Analysis for Cell Surface Markers and Stem Cell Markers

To characterize the phenotype of the cell population, total RNA was extracted from the freshly sorted CD31⁻;CD146⁻ SP cells and CD31⁺;CD146⁻ SP cells using Trizol (Invitrogen Corp.). The number of these cells was normalized to 5×10^4 cells in each experiment. First-strand cDNA syntheses were performed from total RNA by reverse transcription using the SuperScript II preamplification system (Invitrogen Corp.). Real-time reverse transcription-polymerase chain reaction (RT-PCR) amplifications were performed at 95°C for 10 seconds, 62°C for 15 seconds, and 72°C for 8 seconds using macrophage/mononuclear cell markers, *CD11b* and *CD14*, hematopoietic cell marker, *CD45*, angioblast marker, *CD133*, neuronal progenitor marker, *Sox2*, and stem cell markers, *CXCR4*, *Bcrp1*, *Stat3*, *Bmi1*, and *Tert* (supplemental online Table 1 and Iohara et al. [12]) labeled with Light Cycler-Fast Start DNA master SYBR Green I (Roche Diagnostics, Pleasanton, CA, http://www.roche-applied-science.com) in Light Cycler (Roche Diagnostics). The design of the oligonucleotide primers was based on published porcine cDNA sequences. When porcine sequences were not available, human sequences were used. The RT-PCR products were subcloned into pGEM-T Easy vector (Promega, Madison, WI, http://www.promega.com) and confirmed by sequencing based on published cDNA sequences. The expression in CD31⁻;CD146⁻ SP cells and CD31⁺;CD146⁻ SP cells was compared with porcine pulp tissue after normalizing with β-actin.

Proliferation and Migration Assay

To measure proliferation of CD31⁻;CD146⁻ SP cells compared with CD31⁺;CD146⁻ SP cells and CD31⁺;CD146⁺ SP cells, these cells at third passage at the 10^3 cells per 96 well were cultured in EBM2 supplemented with 0.2% bovine serum albumin (Sigma) and bFGF (50 ng/ml; Invitrogen Corp.), VEGF-A (50 ng/ml; Peprotech Ltd., London, http://www.peprotech.com), EGF (50 ng/ml, Invitrogen Corp.), stromal cell-derived factor 1 (SDF1; 50 ng/ml) (Acris, Hiddenhausen, Germany, http://www.acris-antibodies.com), and IGF1 (50 ng/ml; Peprotech Ltd.). Tetracolor one (10 μl) (Seikagaku Kogyo, Co., Tokyo, http://www.seikagaku.co.jp) was added to the 96-well plate, and cell numbers were measured using spectrophotometer at 450 nm absorbance at 0, 12, 24, 36, 48, and 72 hours of culture. Wells without cells served as negative controls.

To examine the migration activity of CD31⁻;CD146⁻ SP cells compared with CD31⁺;CD146⁻ SP cells and CD31⁺;CD146⁺ SP cells, 5×10^4 cells were seeded on PET-membrane (BD Biosciences) inserted into 24-well assembly containing EBM2 supplemented with VEGF-A (Peprotech Ltd.) at the final concentration of 0, 5, 10, and 100 ng/ml. Twenty-four hours later, cells that passed through the membrane were counted after detaching the cells from the membrane with 0.2% trypsin-0.02% EDTA. The migration activity was also examined in the culture with SDF1 (Acris) or granulocyte colony-stimulating factor (G-CSF) (Peprotech Ltd.) and compared with VEGF-A at the final concentration of 50 ng/ml.

Induced Chondrogenic, Adipogenic, Neurogenic, and Odontogenic Differentiation

The differentiation of pulp CD31⁻;CD146⁻ SP cells into adipogenic, chondrogenic, neurogenic, and odontoblastic cells was determined and compared with CD31⁺;CD146⁻ SP cells by the previously described methods [12]. Odontogenic potential in vivo was confirmed 28 days after autologous transplantation in a canine amputated model of pulp injury [13; K.I. manuscript submitted for publication]. The cells were transplanted in the form of a pellet (cellular aggregates) with collagen type I and type III after 1,1'-dioctadecyl-3,3,3',3'-tetramethylindodicarbocyanine perchlorate (DiI) labeling on the amputated pulp.

Endothelial Differentiation In Vitro

The CD31⁻;CD146⁻ SP cells, CD31⁺;CD146⁻ SP cells, and CD31⁺;CD146⁺ SP cells at the third to fifth passage were seeded

on the matrigel (BD Biosciences) in EGM2. Network formation was observed after 24-hour cultivation. The paraffin-embedded sections on day 10 were observed by in situ hybridization analysis [12] using porcine *CEACAM1, CD146*, and *occludin* antisense probes. The DIG-labeled probes were constructed out of the plasmids after subcloning the RT-PCR products into pGEM-T Easy vector using each primer pair (supplemental online Table 2). CD31⁻; CD146⁻ SP cells were cultured for 14 days and then subcultured. The immunocytochemical analyses were performed with primary antibodies, anti-von Willebrand factor (vWF) (1:20) (H-300) (Santa-Cruz, Biotech, Santa Cruz, CA, http://www.scbt.com), anti-CD31 (1:20) (LCI-4) (AbD Serotec Ltd.), and anti-vascular endothelial (VE)-cadherin/CD144 (1:50) (123) (Acris). They were further stained with goat anti-mouse IgG-horseradish peroxidase (HRP) (Invitrogen Corp.) enhanced with TSA system rhodamine-conjugated tyramide (Invitrogen Corp.), goat anti-rabbit IgG-Alexa 568 (Invitrogen Corp.), and goat anti-rat IgG-HRP (GE Healthcare U.K. Ltd., Buckinghamshire, U.K., http://www.gehealthcare.com) enhanced with TSA system Alexa 488-conjugated tyramide (Invitrogen Corp.). The differential changes of expression were analyzed by a fluorescence microscope IX 71 (Olympus, Tokyo http://www.olympus-global.com) after counterstaining with Hoechst 33342.

To detect the endothelial function of histamine-mediated release of vWF, CD31⁻;CD146⁻ SP cells at the third passage were cultured in EGM2 for 14 days. They were further incubated with 10 μM histamine (Sigma) for 60 minutes and stained with an antibody against vWF. The uptake of acetylated-low-density lipoprotein (LDL) (Biomedical Technologies, Inc., Stoughton, MA, http://www.btiinc.com) as an index of endothelial function was examined. The cells derived from CD31⁻;CD146⁻ SP cells (10⁴ cells/ml) at the third passage were cultured in EGM2 for 14 days. On day 17 and day 21, DiI-acetylated-LDL (Biomedical Technologies, Inc.) was added at the final concentration of 10 μg/ml for 2 hours.

Transplantation into Mouse Ischemic Hind Limbs

The potential of neovascularization of porcine pulp CD31⁻; CD146⁻ SP cells and CD31⁺;CD146⁻ SP cells was examined in a murine model of hind limb ischemia in 5-week-old severe combined immunodeficient mice (CB17; CLEA, Tokyo, http://www.clea-japan.com). PBS injection was also used as control. After inhalation anesthesia with isoflurane, the left proximal portion of femoral artery including the superficial and the deep branches and the distal portion of the saphenous artery were ligated as previously described [14]. After 24 hours, 100 μl of PBS with or without 1 × 10⁶ freshly detached CD31⁻;CD146⁻ SP cells or CD31⁺;CD146⁻ SP cells at the third to fifth passage with DiI (Sigma) labeling was injected intramuscularly. Laser Doppler imaging (Perimed AB, Stockholm, Sweden, http://www.perimed.se) was performed 14 days after cell transplantation. The blood vessels were decorated with perfused FITC-conjugated dextran (Sigma). Neovascularization and engraftment of the transplanted cells into the hind limb were examined by confocal microscope using FLUO VIEW FV1000 (Olympus) instrument. Three-dimensional structures were reconstructed by METAMORPH (Molecular Devices, Sunnyvale, CA, http://www.moleculardevices.com) and IMARIS (Bitplane AG, Zurich, Switzerland, http://www.bitplane.com). Isolated muscle tissues of ischemic hind limb were fixed and serial cryotome sections (12 μm) were stained with Fluorescein Griffonia (Bandeiraea) Simplicifolia Lectin 1/fluorescein-galanthus nivalis (snowdrop) lectin (20 μg/ml; Vector Laboratories, Inc., Youngstown, OH, http://www.vectorchemicals.com) to monitor the presence and localization of the transplanted cells in relation to newly formed blood vessels using a fluorescence microscope BIOREVO, BZ-9000 (KEYENCE, Osaka, Japan, http://www.keyence.co.jp). Microscopic digital images of six sections of every 120 μm were scanned in a frame composed of 500 μm × 380 μm rectangle and statistical analyses was performed using software, Dynamic cell count, BZ-HIC (KEYENCE). The experiment was repeated three times. The ultrathin sections of the hamstring muscles embedded in Epon were examined with an electron microscope (model 1010; JEOL, Tokyo, http://www.jeol.com) as previously described [15]. The cryotome

sections obtained on day 7 were observed by in situ hybridization analysis [12] using porcine *G-CSF, granulocyte-macrophage colony-stimulating factor (GM-CSF), matrix metalloprotease (MMP)1, MMP3, VEGF-A,* and *CXCR4* antisense probes. The probes were constructed out of the plasmids after subcloning the PCR products using the same primers designed for real-time RT-PCR (supplemental online Table 1).

Analysis of Gene Expression of Cytokines and Enzymes by Real-Time RT-PCR

The mRNA expression of angiogenic (*VEGF-A, hepatocyte growth factor [HGF]*), chemotactic (*G-CSF, GM-CSF, MCP1, CXCL2, MDCFI, MDCFII, TF*), and proinflammatory (*interleukin [IL]-1α, IL-6, IL-12A, leukemia inhibitory factor [LIF]*) cytokines and matrix-degrading enzymes (*MMP1, MMP2, MMP3, MMP9*) and others (*Arginase I, Lipoprotein lipase, Dipeptidyl peptidase IV, Hyaluronan synthase 2 [SHAS2], parathyroid hormone-like hormone [PTHLH], Integrin β-like protein 1, GP38K,* and *Calcitonin receptor-stimulating peptide [CRSP]*) (supplemental online Table 1) was compared in pulp CD31⁻;CD146⁻ SP cells with those in pulp CD31⁺;CD146⁻ SP cells at third passage of culture by real-time RT-PCR. The RT-PCR products were confirmed by sequencing based on published cDNA sequences. The expression was compared with porcine pulp tissue after normalizing with β-actin.

Proliferation and Antiapoptotic Effect of Pulp CD31⁻;CD146⁻ SP Cell-Conditioned Medium

At 50% confluence, culture medium was switched to EBM2 and the conditioned media from CD31⁻;CD146⁻ SP cells and CD31⁺; CD146⁻ SP cells were collected 48 hours later. Human umbilical vein endothelial cells (HUVECs) (KURABO Industries, Osaka, Japan, http://www.kurabo.co.jp) were cultured in EGM2 containing 2% fetal bovine serum (FBS) for 24 hours and further in EBM2 containing 0.2% bovine serum albumin (BSA) for 24 hours. Then, the medium was changed into EBM2 containing 2% FBS supplemented with 20% of conditioned medium from pulp CD31⁻; CD146⁻ SP cells and CD31⁺;CD146⁻ SP cells. Cell numbers were measured by Tetra-color one. The proliferation effects of these conditioned media were compared with those of MMP3 (Millipore, Billerica, MA, http://www.millipore.com), VEGF-A (Peprotech Ltd.), G-CSF (Peprotech Ltd.), and GM-CSF (Peprotech Ltd.) at final concentration of 50 ng/ml. Data were expressed as means ± SD at four determinations. To assess the effect of the conditioned medium of CD31⁻;CD146⁻ SP cells on apoptosis, HUVECs at passage six or less were grown in EGM2 in 35-mm dish for 3 days and then incubated with 100 nM staurosporine (Sigma) in EBM2 supplemented with 20% of conditioned medium from CD31⁻;CD146⁻ SP cells and CD31⁺;CD146⁻ SP cells. As controls, MMP3, VEGF-A, G-CSF, and GM-CSF were added to the EBM2. After 8 hours, HUVECs were harvested, and the cell suspensions were treated with Annexin V-FITC (Roche Diagnostics) and propidium iodide for 15 minutes, and analyzed by flow cytometry. Data were expressed as means ± SD at three determinations.

Statistical Analyses

Data are reported as means ± SD. *P* values were calculated using the unpaired Student's *t* test. The number of replicates in each experiment is indicated in the figure legends.

RESULTS

Isolation of CD31⁻; CD146⁻ SP Cells from Dental Pulp

Flow cytometric analyses of the SP cells from porcine adult pulp tissues were performed using antibodies against CD31 and CD146 to isolate further distinct subpopulations. CD31 is known to be highly expressed in endothelial progenitor cells and

STEM CELLS
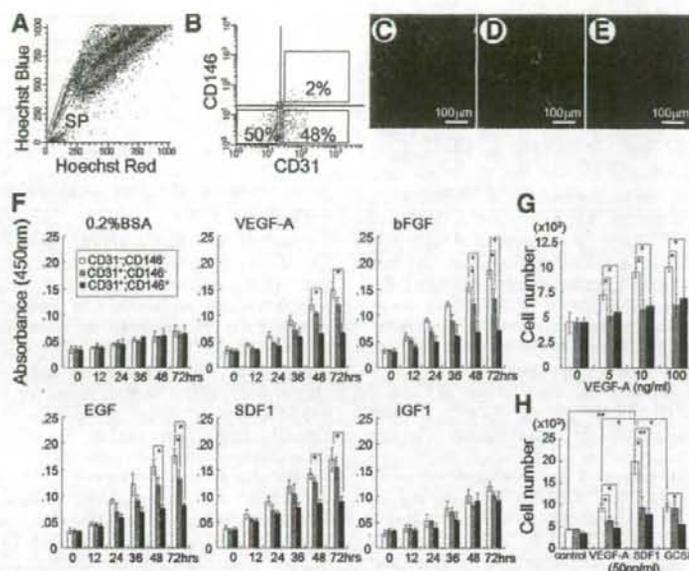
Figure 1. Isolation and comparison of proliferation and migration activities of subfractions of CD31$^-$;CD146$^-$, CD31$^+$;CD146$^-$, and CD31$^+$;CD146$^+$ side population (SP) cells from porcine adult dental pulp. **(A):** Flow cytometric analyses of the SP cells. Pulp cells isolated from porcine adult pulp tissues identify approximately 0.2% population with relatively lower Hoechst 33342 fluorescence (SP cells). **(B):** Isolation of further distinct populations from porcine pulp SP cells using antibodies against CD146, CD31 and CD146. CD31$^-$;CD146$^-$, CD31$^+$;CD146$^-$, and CD31$^+$;CD146$^+$ SP cells represented 50%, 48%, and 2%, respectively, of the total. The experiment was repeated ten times, and one representative experiment is presented. **(C, D):** Primary cell culture on day 7. **(C):** CD31$^-$;CD146$^-$ SP cells containing a stellate cell with long processes and a spindle-shaped cell. **(D):** Endothelial-like CD31$^+$;CD146$^-$ SP cells. **(E):** CD31$^+$; CD146$^+$ SP cells showing irregularly shaped cells with a short process. **(F):** The proliferation activity with 0.2% BSA as a control, VEGF-A, bFGF, EGF, and (IGF1) at the final concentration of 50 ng/ml. Cell numbers were determined at 0, 12, 24, 36, 48, and 72 hours of culture. Data are expressed as means ± SD at four determinations (∗, $p < .01$). **(G):** The migration activity with VEGF-A at the final concentration of 0, 5, 10, and 100 ng/ml. Data were expressed as means ± SD at four determinations (∗, $p < .01$). **(H):** The migration activity with VEGF-A, SDF1, and G-CSF. SDF1 induced a stronger response than VEGF-A in CD31$^-$;CD146$^-$ SP cells. Data were expressed as means ± SD at four determinations (∗, $p < .01$; ∗∗, $p < .001$). **(F–H):** Statistical analysis was performed by the nonpaired Student's t test. The experiments were repeated three times and one representative experiment is presented. Abbreviations: bFGF, basic fibroblast growth factor; BSA, bovine serum albumin; EGF, epidermal growth factor; G-CSF, granulocyte colony-stimulating factor; IGF1, insulin-like growth factor 1; SDF1, stromal cell-derived factor 1; VEGF-A, vascular endothelial growth factor A.

endothelial cells and CD146, in smooth muscle cells and endothelial cells. The CD31$^-$ population was devoid of CD146$^+$ and represented 50% of total SP cells. The CD31$^+$ population contained both CD146$^-$ and CD146$^+$ cells, and CD31$^+$;CD146$^+$ and CD31$^+$;CD146$^-$ represented 2% and 48% of total SP cells, respectively (Fig. 1A, 1B). The CD31$^-$;CD146$^-$ SP cells contained two types of cells: a stellate cell with long processes and a spindle-shaped cell. The stellate cells contained a large nucleus with nucleoli. The spindle-shaped cell was neuron-like cell with a long slender process and sparse cytoplasm (Fig. 1C). CD31$^-$;CD146$^-$ SP cells were endothelial-like cells, which grew clonally and were contact inhibited (Fig. 1D). CD31$^+$; CD146$^+$ SP cells were irregularly shaped with short processes (Fig. 1E). To maintain the phenotype of CD31$^-$;CD146$^-$ SP cells EBM2 supplemented with IGF1, EGF, and 10% porcine serum was used, and EBM2 with bFGF, VEGF, and 2% porcine serum was used for CD31$^+$;CD146$^-$ SP cells.

The single CD31$^-$;CD146$^-$ SP cell plated in 35-mm collagen type I-coated dish formed a colony in 8 days (data not shown), showing colony formation activity of these cells. The efficiency of attachment and growth of CD31$^-$;CD146$^-$ SP cells was estimated to be 8.9%, whereas for CD31$^+$;CD146$^-$ SP cells it was 7.7%. Limiting dilution analysis at third passage culture showed that the frequency of colony-forming unit in CD31$^-$;CD146$^-$ SP cells was estimated to be 80%, whereas that in CD31$^+$;CD146$^-$ SP cells was 30%.

www.StemCells.com

Cell Surface Antigen Markers for Stem Cells

To characterize the "stemness," hematopoietic lineage, and endothelial lineage of the porcine pulp CD31$^-$ SP cells and CD31$^+$ SP cells, cell surface antigen markers were examined by flow cytometry and compared with CD31$^-$ SP cells and CD31$^+$ SP cells derived from porcine bone marrow. Markers of monocyte/macrophage origin, CD11b and CD14 were negative in pulp CD31$^-$ SP cells and CD31$^+$ SP cells. Few pulp CD31$^-$ SP cells and CD31$^+$ SP cells expressed CD90, and none expressed CD117/c-kit or CD150 (supplemental online Table 3), whereas CD31$^-$ SP cells derived from porcine bone marrow expressed those at the ratio of 0%, 100%, and 1%, respectively (data not shown). Pulp CD31$^-$ SP cells expressed CD34 and VEGFR2/Flk1 mRNA and proteins (supplemental online Tables 3, 4) and no *CD133* mRNA (supplemental online Table 4), suggesting that pulp CD31$^-$;CD146$^-$ SP cells were similar but not identical to bone marrow-derived endothelial progenitor cells. It is noteworthy that 94% of pulp CD31$^-$;CD146$^-$ SP cells expressed CD271/LNGFR, a marker of neuronal progenitor cells (supplemental online Table 3). *Sox2* mRNA was highly expressed in CD31$^-$;CD146$^-$ SP cells compared with CD31$^+$; CD146$^-$ SP cells (supplemental online Table 4), suggesting a neurogenic population in the former.

Expression of stem cell markers *CXCR4*, *Stat3*, *Bmi1*, and *Tert* mRNA was 8, 1.3, 1.5, and 37.5 times higher, respectively, in CD31$^-$;CD146$^-$ SP cells than those in CD31$^+$;CD146$^-$ SP cells

detected by real-time RT-PCR (supplemental online Table 4). Lack of *CD11b*, *CD14*, and *CD45* mRNA expression in CD31⁻; CD146⁻ SP cells was also confirmed (supplemental online Table 4), suggesting that they are neither of monocyte/macrophage origin nor of hematopoietic lineage.

Proliferation Activity and Chemotaxis of CD31⁻; CD146⁻ SP Cells

We first examined the proliferation activity of pulp CD31⁻; CD146⁻ SP cells and compared them with CD31⁺;CD146⁻ SP cells and CD31⁺;CD146⁺ SP cells. In the presence of 0.2% BSA without serum, all three cell populations proliferated similarly, doubled in 3 days. There is a progressive increase with time in the response to the various factors. Treatment with VEGF-A, bFGF, EGF, and SDF1 singly enhanced proliferation of CD31⁻;CD146⁻ SP cells and CD31⁺;CD146⁻ SP cells almost three times and two times more, respectively, compared with control 0.2% BSA on day 3 (Fig. 1F). IGF1 was less effective in proliferation of CD31⁻; CD146⁻ SP cells and CD31⁺;CD146⁻ SP cells but more effective in proliferation of CD31⁺;CD146⁺ SP cells compared with other growth factors (Fig. 1F).

VEGF-A (100 ng/ml) induced a chemotactic response in a dose-dependent manner in CD31⁻;CD146⁻ SP cells, and induced 1.6 and 1.4 times more strongly than that in CD31⁺; CD146⁻ SP cells and CD31⁺;CD146⁺ SP cells, respectively (Fig. 1G). SDF1 at the final concentration of 50 ng/ml also induced a two times stronger response than VEGF-A (Fig. 1H).

Multilineage Differentiation Potential Capability of SP Cells

The chondrogenic potential of CD31⁻;CD146⁻ SP cells and CD31⁺;CD146⁻ SP cells was examined in both chondrogenic and control media. The porcine pulp CD31⁻;CD146⁻ SP cells and CD31⁺;CD146⁻ SP cells from the fourth passage culture were maintained in pellet cultures for 30 days. The amount of cartilage proteoglycan stained with Alcian Blue was stronger in the pellets induced from CD31⁻;CD146⁻ SP cells compared with those from CD31⁺;CD146⁻ SP cells (Fig. 2A, 2B). The expression of chondrogenic markers *aggrecan* and *type II collagen* mRNA was much stronger in CD31⁻;CD146⁻ SP cells than in CD31⁺; CD146⁻ SP cells and SP cells 14 days after induction (data not shown). However, the expression of *type II collagen* (Fig. 2C) was similar in the two subfractions 21 days after induction. In control media there were no chondrocytes (Fig. 2C).

The adipogenic potential was examined in the third passage cultures that were cultured in adipogenic media for 28 days. Both CD31⁻;CD146⁻ SP cells and CD31⁺;CD146⁻ SP cells showed staining with oil red O (Fig. 2D, 2E), but in control media no staining was observed. Adipogenic markers *aP2* and *PPARγ* mRNA were expressed in the CD31⁻;CD146⁻ SP cells and CD31⁺;CD146⁻ SP cells on day 28 in adipogenic media (Fig. 2F).

Next, the neurogenic potential was determined. Clusters of proliferating neurospheres were more prevalent in the CD31⁻; CD146⁻ SP cells compared with CD31⁺;CD146⁻ SP cells (Fig. 2G, 2H). *Sox2* mRNA expression was similar in both groups (Fig. 2I). The neurospheres from both fractions were immuno-reactive for neuromodulin 14 days after induction (Fig. 2J, 2K). The expression of neural markers *neuromodulin*, *neurofilament*, and *sodium channel, voltage-gated, type Iα (ScnIA)* mRNA was similar in the CD31⁻;CD146⁻ SP cells as that in the CD31⁺; CD146⁻ SP cells (Fig. 2L).

Finally, differentiation of CD31⁻;CD146⁻ SP cells into odontoblast lineage was examined. The mineralized matrix was stained by alizarin red in both CD31⁻;CD146⁻ SP cells and CD31⁺;CD146⁻ SP cells 28 days after induction in vitro (Fig. 2M, 2N). The DiI-labeled CD31⁻;CD146⁻ SP cells that at-

tached to the dentinal wall in the cavity on the amputated pulp differentiated into odontoblasts and formed tubular dentin 28 days after autologous transplantation in the cavity on the canine amputated pulp in vivo (Fig. 2O–2Q). The mRNA expression of odontoblast markers, *Dspp* and *enamelysin*, was similar in CD31⁻;CD146⁻ SP cells and CD31⁺;CD146⁻ SP cells 14 days after induction in pellet culture (Fig. 2R).

Differentiation of CD31⁻;CD146⁻ SP Cells into Endothelial Cells

The endothelial differentiation potential was assessed. CD31⁻; CD146⁻ SP cells readily formed extensive networks of cords and tube-like structures as early as 12 hours (Fig. 3A), a phenotype typically associated with endothelial cells, suggesting an angioblast phenotype. On the other hand, CD31⁺;CD146⁻ SP cells and CD31⁺;CD146⁺ SP cells formed only short strands (Fig. 3B, 3C). Capillary-like structures were also observed in cells cultured in matrigel (Fig. 3D). In situ hybridization analysis showed mRNA expression of *CEACAM1* (Fig. 3E), *CD146* (Fig. 3F), and *Occludin* (Fig. 3G), markers for endothelial cells.

We also examined whether CD31⁻;CD146⁻ SP cells can differentiate into endothelial cells in monolayer culture. In the EBM2 supplemented with 2% porcine serum and 10 ng/ml VEGF-A and 10 ng/ml bFGF, endothelial marker vWF (Fig. 3H, 3K) was detected by immunocytochemistry in 3 days, whereas expression of CD31 (Fig. 3I, 3L) and VE-cadherin (Fig. 3J, 3M), a marker of more mature endothelial cells, was observed after 10 days and 21 days of culture, respectively.

Next, functional characteristics of endothelial cells induced from CD31⁻;CD146⁻ SP cells with VEGF-A were investigated. In vitro release of vWF is stimulated by histamine treatment. vWF was distributed throughout the cytoplasm prior to histamine treatment and much decreased after treatment (Fig. 3N, 3O). The uptake of acetylated-LDL in CD31⁻;CD146⁻ SP cells was high on day 21 (Fig. 3P, 3Q).

CD31⁻;CD146⁻ SP Cells Induce Functional Neovascularization in Ischemic Hind Limb

Fourteen days after transplantation of CD31⁻;CD146⁻ SP cells (Fig. 4A, 4D), the quantitative analysis of laser Doppler imaging revealed that the blood flow was significantly increased 1.3 and 1.6 times more in the ischemic hind limb compared with CD31⁺;CD146⁻ SP cells (Fig. 4B, 4D) and PBS control without cells (Fig. 4C, 4D), respectively. Capillary density was increased in the ischemic hind limb after transplantation of CD31⁻;CD146⁻ SP cells (Fig. 4E), to a greater extent compared with CD31⁺;CD146⁻ SP cells (Fig. 4F) and PBS control (Fig. 4G). Quantitative analysis using serial sections revealed that capillary density in the ischemic region transplanted with CD31⁻;CD146⁻ SP cells increased 13-fold higher than that with CD31⁺;CD146⁻ SP cells (Fig. 4H–4K). Semithin sections of the ischemic lesion of transplantation of CD31⁻;CD146⁻ SP cells (Fig. 4L) demonstrated numerous migrating cells among newly formed capillaries. Electron micrographs showed that intact capillaries with basement membrane and pericytes were surrounded by the migrating cells (Fig. 4M). Capillaries were functional with complete lumens. The migrating cells surrounding these intact capillaries were rich in cytoplasmic organelles with irregularly shaped nuclei. They were unlike the inflammatory polymorphonuclear cells or scavenging mononuclear cells (Fig. 4N). Confocal laser micrographs showed that CD31⁻;CD146⁻ SP cells were present in close proximity to the vessel (Fig. 4O, 4P), suggesting they migrated to the ischemic region and stimulated neovascularization rather than functionally incorporating into vessels (Fig.

STEM CELLS
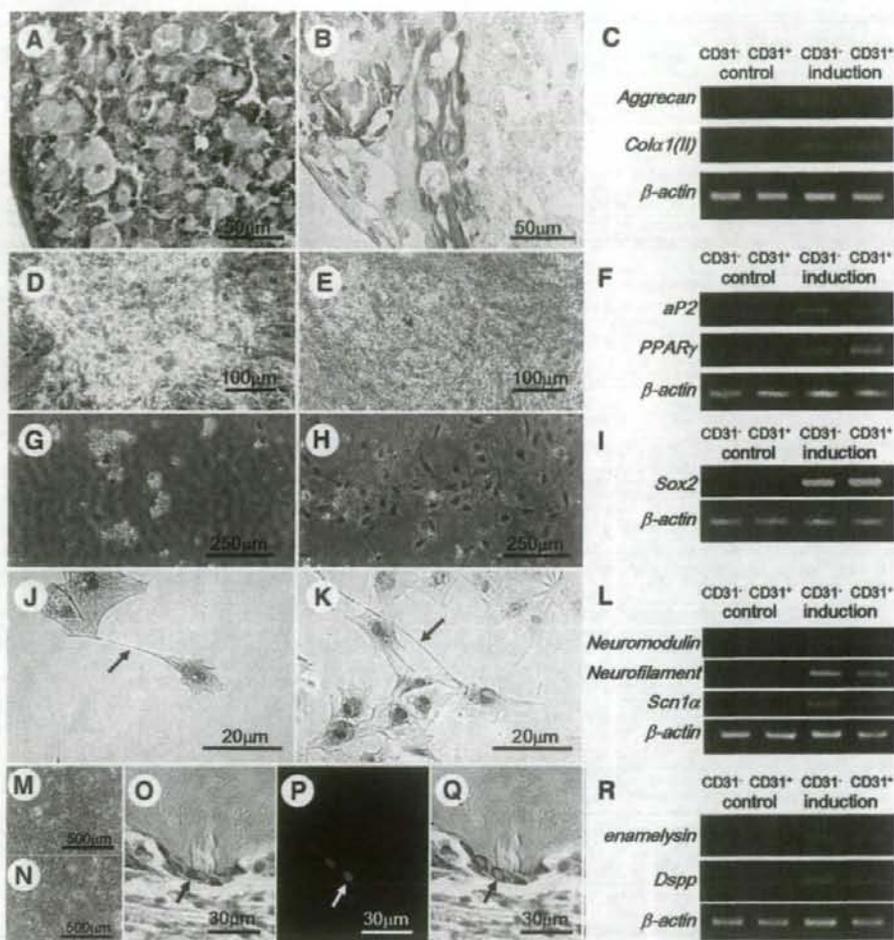
Figure 2. Multilineage differentiation potential of subfractions of CD31⁻;CD146⁻ and CD31⁺;CD146⁻ side population (SP) cells. The experiment was repeated three times, and one representative experiment is presented. (A–C): Chondrogenic potential. (A, B): Thirty days after induction of fourth passage cell populations. (A): CD31⁻;CD146⁻ SP cells; (B) CD31⁺;CD146⁻ SP cells, Alcian Blue staining. (C): Expression of *Aggrecan* and *Collagen αl(II)* mRNA 21 days after induction. (D–F): Adipogenic potential. Twenty-eight days after induction of third passage cell populations. (D): CD31⁻;CD146⁻ SP cells; (E) CD31⁺;CD146⁻ SP cells, oil red O staining. (F): Expression of *aP2* and *PPARγ* mRNA. (G–I): Neurosphere formation. Fifteen days after induction of third passage cell populations. (G): CD31⁻;CD146⁻ SP cells. (H): CD31⁺;CD146⁻ SP cells. (I): *Sox2* mRNA expression in the neurospheres from CD31⁻;CD146⁻ SP cells and from CD31⁺;CD146⁻ SP cells. (J–L): Neuronal potential. Fourteen days after induction of dissociated neurosphere cells from (J) CD31⁻;CD146⁻ SP cells and (K) CD31⁺;CD146⁻ SP cells. Immunostaining with neuromodulin. (L): *Neuromodulin, neurofilament,* and *sodium channel, voltage-gated, type Iα (ScnIA)* mRNA expression in CD31⁻;CD146⁻ SP cells compared with CD31⁺;CD146⁻ SP cells. (M–R): Odontogenic potential. (M, N): Twenty-eight days and (R) fourteen days after induction with ascorbic acid and Pi to a 4-mM final concentration in pellet culture. (M): CD31⁻;CD146⁻ SP cells; (N) CD31⁺;CD146⁻ SP cells. Alizarin red staining. (O–Q): Twenty-eight days after autologous transplantation of the 1,1'-dioctadecyl-3,3,3',3'-tetramethylindocarboeyanine perchlorate-labeled CD31⁻;CD146⁻ SP cells in the canine amputated pulp in vivo. Note differentiation into odontoblasts (arrows). (O): H&E staining. (P): DiI immunofluorescent image. (Q): Merge. (R): Expression of *enamelysin* and *Dspp* mRNA.

4O). However, CD31⁺;CD146⁻ SP cells were not in close proximity of the vessels (Fig. 4Q).

Analysis of Gene Expression

The expression of angiogenic (*VEGF-A, HGF*), chemotactic (*G-CSF, GM-CSF, MCP1, CXCL2, MDCFI, MDCFII, TF*), and proinflammatory (*IL-1α, IL-6, LIF*) cytokines, matrix-degrading enzymes (*MMP1, MMP3, MMP9*), and others (*Arginase I, Lipoprotein lipase, Dipeptidyl peptidase IV, Hyaluronan synthase*

2, *GP38K* and *CRSP*) was stronger in CD31⁻;CD146⁻ SP cells compared with CD31⁺;CD146⁻ SP cells (Table 1). *G-CSF, GM-CSF, MMP1, MMP3, VEGF-A,* and *CXCR4* were expressed in the DiI-labeled CD31⁻;CD146⁻ SP cells in the ischemic region 7 days after transplantation (Fig. 5). The conditioned medium of CD31⁻; CD146⁻ SP cells showed mitogenic (Fig. 6A) and antiapoptotic activities on HUVECs as MMP3, VEGF-A, and G-CSF (Fig. 6B). Thus, these results imply paracrine actions of proangiogenic and chemotactic cytokines in promoting neovascularization.
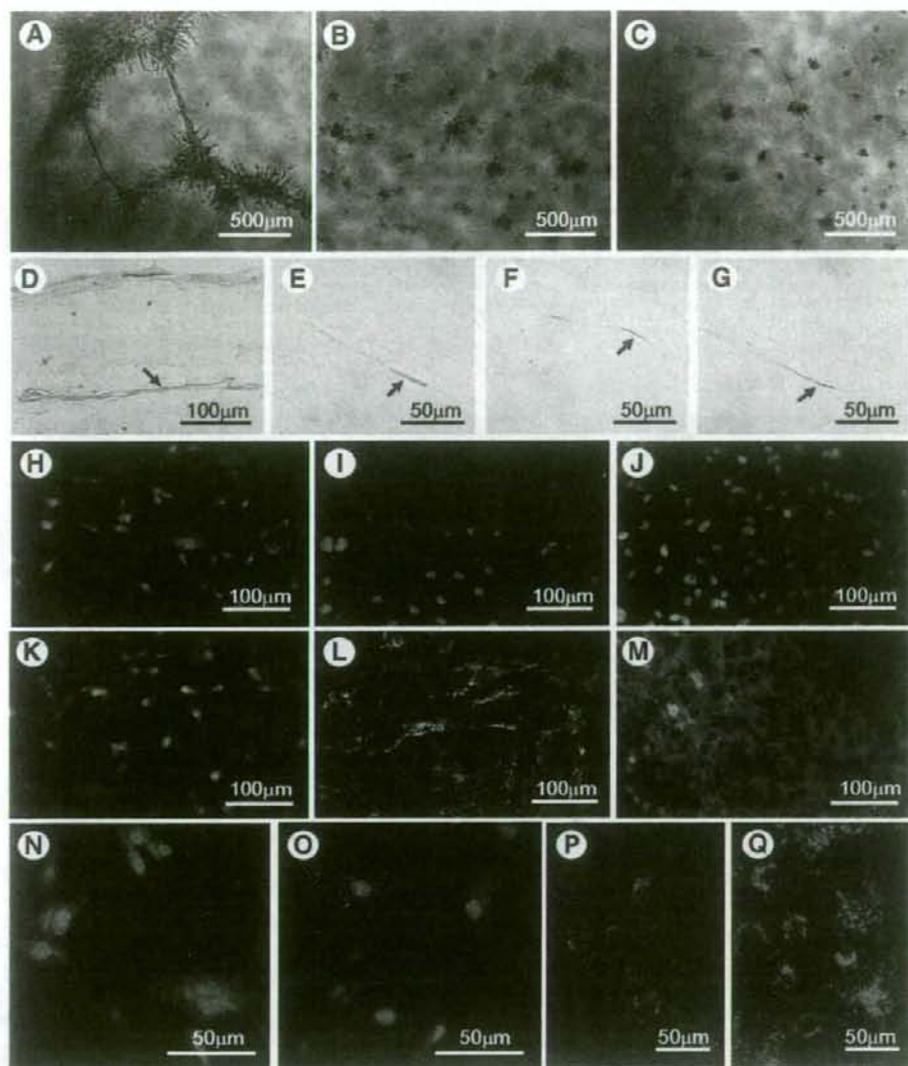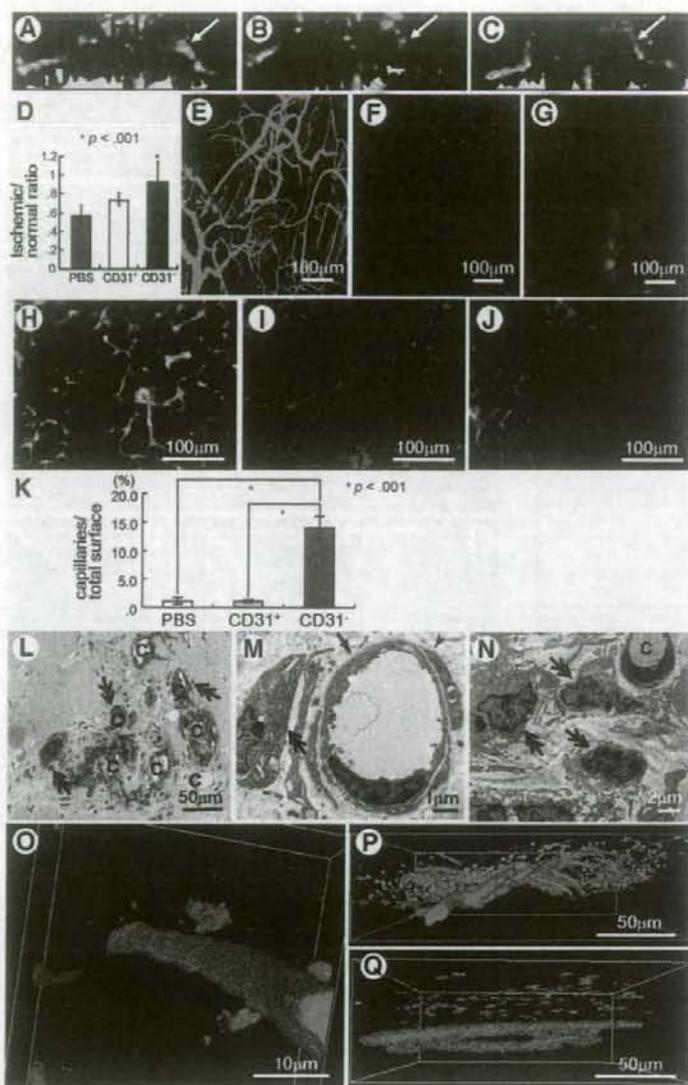
Figure 3. Differentiation of CD31⁻;CD146⁻ side population (SP) cells into endothelial cells in vitro. The experiment was repeated three times, and one representative experiment is presented. **(A–G):** The endothelial differentiation potential using the matrigel assay. **(A–C):** Twelve hours after seeding. Extensive networks of cords and tube-like structures in **(A)** CD31⁻;CD146⁻ SP cells. Smaller number of cords in **(B)** CD31⁺;CD146⁻ SP cells and **(C)** CD31⁺;CD146⁺ SP cells. **(D–G):** Capillary formation after seeding of CD31⁻;CD146⁻ SP cells at 10 days. **(D):** H&E staining. Note the capillary structure in the matrigel. In situ hybridization analysis of the markers for endothelial cells. **(E)** *CEACAM1*, **(F)** *CD146*, and **(G)** *Occludin*. Arrows show positive signals along the capillary structure. **(H–M):** Differentiation of CD31⁻;CD146⁻ SP cells into endothelial cells in monolayer culture in the presence of 2% porcine serum and 10 ng/ml vascular endothelial growth factor A and 10 ng/ml basic fibroblast growth factor. Immunocytochemistry of **(H, K)** von Willebrand factor (vWF), **(I, L)** CD31, and **(J, M)** vascular endothelial (VE)-cadherin. **(H–J):** Three days, **(K, L)** 10 days, and **(M)** 21 days of culture. Note vWF detected on day 3 and day 10; CD31, on day 10; and VE-cadherin, on day 21. **(N–Q):** Functional characteristics of endothelial cells induced from CD31⁻;CD146⁻ SP cells. **(N):** Before treatment with histamine. **(O):** After treatment with histamine, vWF was released. Uptake of acetylated-low-density lipoprotein by cells 17 days after induction **(P)** and 21 days after induction **(Q)**.

DISCUSSION

The present investigation focused on subfractionation of SP cells from porcine dental pulp into CD31⁻; CD146⁻ and CD31⁺;

CD146⁻ cells and assessment of their multilineage differentiation with special reference to vasculogenesis. There is increasing evidence of multilineage differentiation of tissue stem cells including SP cells. Previous work has demonstrated that SP cells from porcine dental pulp differentiated into adipocytes, chondrocytes,

STEM CELLS

Figure 4. Neovascularization in ischemic hind limb 14 days after transplantation of CD31⁻;CD146⁻ side population (SP) cells compared with CD31⁺;CD146⁻ SP cells. (A–C): Laser Doppler imaging. The experiment was repeated five times, and one representative experiment is presented. (A): CD31⁻;CD146⁻ SP cells, (B) CD31⁺;CD146⁻ SP cells, and (C) PBS control without cells. Arrows show blood flow in the ischemic region. (D): Quantification of blood flow in ischemic versus control limbs obtained from five mice in each group. Statistical analysis was performed by the nonpaired Student's *t* test. (E–G): Confocal laser microscopic analysis after perfusion labeling with fluorescein isothiocyanate-dextran in the muscles of the ischemic hind limb. Transplantation of (E, H) CD31⁻; CD146⁻ SP cells, (F, I) CD31⁺;CD146⁻ SP cells, and (G, J) PBS control. (H–J): Stained with BS1-lectin and Hoechst 33342. (K): Statistical analysis using serial sections. Capillary density in the ischemic region significantly increased in transplantation of CD31⁻;CD146⁻ SP cells compared with PBS control and CD31⁺;CD146⁻ SP cells. (L–N): Electronmicroscopic analysis of the ischemic lesion in transplantation of CD31⁻; CD146⁻ SP cells. (L): Semithin section with toluidine blue staining showing lots of migrating cells (double arrows) among newly formed capillaries (C) in the intramuscular connective tissue. (M): Electronmicrogram showing intact capillaries with basement membrane (arrow) and a pericyte (arrowhead) surrounded by the migrating cells (double arrows) of the ischemic legion. (N): Migrating cells (double arrows) surrounding an intact capillary (C). (O–Q): Three-dimensional confocal laser micrograph. (O, P): 1,1'-dioetadeeyl-3,3,3',3'-tetramethylindocarboeyanine perchlorate (DiI)-labeled CD31⁻;CD146⁻ SP cells present in the proximity of the vessel. (Q): DiI-labeled CD31⁺;CD146⁻ SP cells separated from the vessels. (E–Q): The experiment was repeated three times, and one representative experiment is presented. Abbreviation: PBS, phosphate-buffered saline.

neuronal cells, and odontoblasts [12]. Subfractionation of SP cells into CD31⁻;CD146⁻ and CD31⁺;CD146⁻ cells demonstrated that the former subfraction formed more neurospheres and expressed neurogenic marker CD271, suggesting a stronger neurogenic potential in CD31⁻;CD146⁻ SP cells. On the other hand, the adipogenic, chondrogenic, and odontogenic differentiation potential was similar in the two subfractions of SP cells.

It is well known that bone marrow and peripheral blood contain EPCs with properties of embryonic angioblasts with potential to differentiate into mature endothelial cells [4, 16–18]. The early angioblasts and EPCs express CD34, CD133, and VEGFR2. The expression of CD133 declines and that of CD146 increases in the differentiated endothelial cells [19, 20]. During maturation of bone marrow angioblasts to early EPCs, CD31 is expressed [21]. In

www.StemCells.com

human embryonic aorta [6] and human adult vascular wall [7], the endothelial progenitors are CD34⁺ and CD31⁻. The adipose tissue-derived stromal-vascular fraction also contains CD34⁺;CD31⁻ cells [8]. It is noteworthy that the porcine pulp SP subfraction, CD31⁻;CD146⁻ SP cells expressed CD34 and VEGFR2 as in EPCs. However, they lacked CD11b, CD14, and CD45, demonstrating that these cells are distinct from the hematopoietic lineage. In addition, it is noteworthy that pulp CD31⁻;CD146⁻ SP cells did not express *CD133* mRNA unlike the adipose tissue- and bone marrow-derived EPCs. Thus, the porcine pulp CD31⁻;CD146⁻ SP cells are similar but not identical to EPCs and expressed stem cell markers, *CXCR4, Stat3, Bmi1,* and *Tert.*

Vasculogenic potential of CD34⁺;VEGFR2⁺;CD133⁺; CD90⁺ stem cells derived from human dental pulp has been

Table 1. Relative mRNA expression of cytokines and enzymes by real-time reverse transcription-polymerase chain reaction in CD31⁻;CD146⁻ side population (SP) cells, pulp CD31⁺ SP cells

	CD31⁻;CD146⁻ SP / pulp tissue	CD31⁺;CD146⁻ SP / pulp tissue
VEGF-A	154.3	65.3
HGF	1.0	0.1
G-CSF	26.9	0.2
GM-CSF	1260.7	1.2
MCP1/CCL2	30.3	0.6
CXCL2	26.9	0.1
MDCF I	1243.3	21.6
MDCF II	2033.9	0.1
TF	42.2	0.8
SDF1	1.2	23.9
IL-1α	229.1	2.7
IL-6	257.8	4.5
IL-12ᵃ	0.2	1.0
LIF	128.0	1.7
MMP1	3281.2	0.8
MMP2	1.4	0.7
MMP3	61.4	0.0
MMP9	1.3	0.2
Arginase 1	68.1	3.6
Lipoprotein lipase	4.5	0.1
Dipeptidyl peptidase IV	1.1	0.0
SHAS2	30.7	0.3
PTHLH	0.6	0.0
Integrin, beta-like 1	12.7	0.3
GP38K	657.1	0.1
CRSP	50.2	0.1

ᵃThe value is expressed as relative expression to that in CD31⁺; CD146⁻ SP cells, since the pulp tissue did not express IL-12.

reported in the induced bone tissue after subcutaneous transplantation [22] and in myocardial infarction [23]. In the present study, the functional ability of neovascularization of CD31⁻; CD146⁻ SP cells was determined and demonstrated to form extensive networks of cords and tube-like structures on matrigel. On the other hand, CD31⁺;CD146⁻ SP cells were feeble in cord formation. Treatment of CD31⁻;CD146⁻ SP cells with VEGF-A and bFGF resulted in VE-cadherin expression, histamine-induced vWF release, and uptake of acetylated-LDL, all hallmarks of endothelial differentiation. In addition, CD31⁻;CD146⁻ SP cells exhibited neovascularization in the mouse hind limb ischemia model.

After injury, endothelial cells increase expression of VEGF, which induces SDF1 in the perivascular fibroblasts. SDF1 mobilizes CXCR4-positive cells to the perivascular site where they act in a paracrine fashion to enhance proliferation of resident endothelial cells [24]. The regeneration potential for dentin-pulp complex in response to pulp injury may be attributed to pulp stem/progenitor cells migrating from perivascular region in the pulp tissue deeper from the injured site [25]. The proangiogenic signals such as VEGF released from injured dental pulp cells [26] and endothelial cells [27] or from carious dentin [28] provide chemotactic signals to recruit pulp stem/progenitor cells in pulp tissue. CD31⁻;CD146⁻ SP cells showed higher expression of CXCR4 compared with CD31⁺;CD146⁻ SP cells. CD31⁻;CD146⁻ SP cells were in proximity of vessel and close to neighboring cells expressing SDF1 (data not shown). CD31⁺;CD146⁻ SP cells were at a distance from it in the ischemia model. CD31⁻;CD146⁻ SP cells exhibits high migration activity by VEGF and SDF1 compared with CD31⁺; CD146⁻ SP cells in the chemotaxis experiment. These results imply SDF1/CXCR4 system for migration of pulp CD31⁻; CD146⁻ SP cells in the ischemic region.
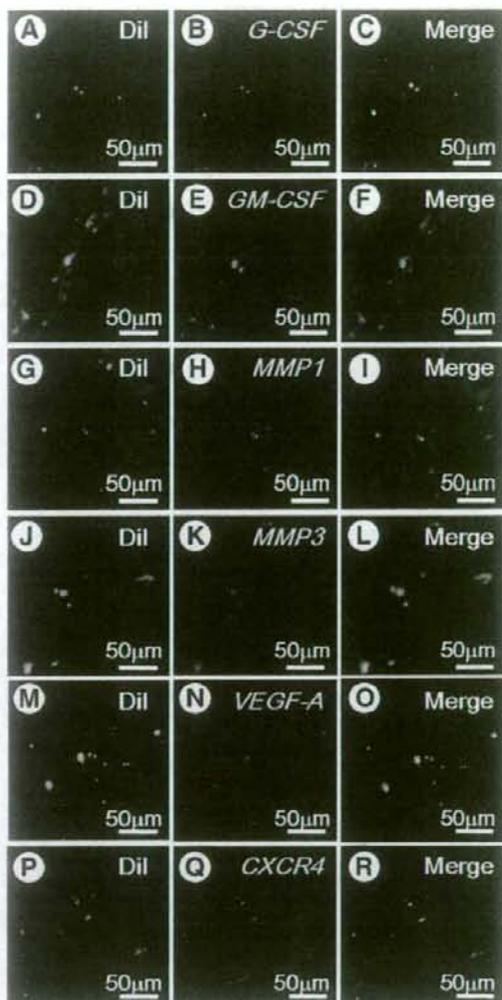
Figure 5. Analysis of gene expression by in situ hybridization. The experiment was repeated three times, and one representative experiment is presented. (A–C): G-CSF, (D–F) GM-CSF, (G–I) MMP1, (J–L) MMP3, (M–O) VEGF-A, and (P–R) CXCR4 mRNA are expressed in the 1,1'-dioetadeeyl-3,3,3',3'-tetramethylindocarboeyanine perchlorate (DiI)-labeled CD31⁻;CD146⁻ side population (SP) cells transplanted in the mouse hind limb ischemic region 7 days after transplantation.

It is important to note these CD31⁻;CD146⁻ SP cells compared with CD31⁺;CD146⁻ SP cells expressed more VEGF-A, G-CSF, and GM-CSF. G-CSF promotes endothelial migration and tubule formation in vitro, and local injection of G-CSF effectively augments ischemia-induced angiogenesis in vivo [29]. GM-CSF induces vascular proliferation and improves blood flow in coronary artery disease and cerebral artery occlusion [30–32]. MMPs are involved in degrading extracellular matrix and basement membrane structures, allowing endothelial migration to occur. MMPs also promote the release of extracellular matrix-bound cytokines, such as VEGF, which can promote proliferation of EPCs and endothelial cells and

STEM CELLS
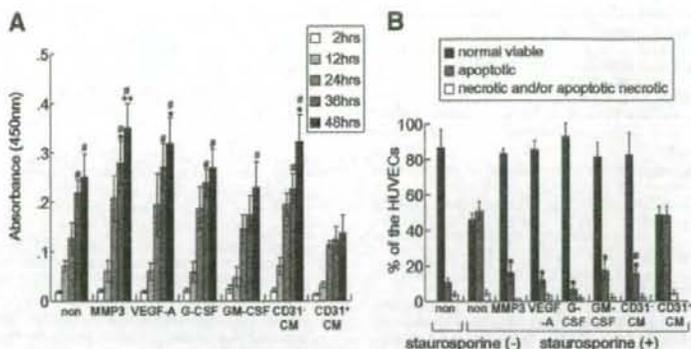
Figure 6. The mitogenic and antiapoptotic activity of conditioned medium of pulp CD31⁻;CD146⁻ side population (SP) cells on endothelium. Data were expressed as means ± SD at four determinations. The experiment was repeated three times, and one representative experiment is presented. Statistical analysis was performed by the nonpaired Student's t test. (A): The proliferation activity of the CM of CD31⁻;CD146⁻ SP cells compared with MMP3, VEGF-A, G-CSF, and GM-CSF and CM of CD31⁺;CD146⁻ SP cells on human umbilical vein endothelial cells (HUVECs) at 2, 12, 24, 36, and 48 hours of culture with Tetra-color one. Note the significant increase with CM of CD31⁻;CD146⁻ SP cells as well as those with cytokines compared with CM of CD31⁺;CD146⁻ SP cells (#, $p < .01$) at 36 and 48 hours. ∗∗, $p < .01$; ∗, $p < .05$ versus control. (B): The relative percentages of viable, apoptotic, and "apoptotic necrotic" or necrotic HUVECs analyzed by flow cytometry. In the presence of 100 nM staurosporine, the CM of pulp CD31⁻;CD146⁻ SP cells had significant antiapoptotic effect as MMP3, VEGF-A, G-CSF, and GM-CSF compared with control (∗, $p < .01$), and higher effect compared with the CM of pulp CD31⁺;CD146⁻ SP cells (#, $p < .01$). Abbreviations: CM, conditioned medium; G-CSF, granulocyte colony-stimulating factor; GM-CSF, granulocyte-macrophage colony-stimulating factor; MMP3, matrix metalloprotease 3; VEGF-A, vascular endothelial growth factor A.

regulate angiogenesis [33–36]. The higher gene and protein expression of MMP3 by pulp-derived CD31⁻;CD146⁻ SP cells compared with CD31⁺;CD146⁻ SP cells is noteworthy and may explain the anticipated invasive behavior during endothelial migration [33, 37, 38]. The conditioned medium of pulp-derived CD31⁻;CD146⁻ SP cells enhanced proliferation and survival rate of HUVECs, suggesting the paracrine role of CD31⁻; CD146⁻ SP cells on local vascular cells to create a permissive environment that enables rapid revascularization, proliferation, and survival of damaged cells [39, 40]. The isolation of EPCs from bone marrow, umbilical cord blood, peripheral blood, and adipose tissue is documented. To this list of sources of EPCs now dental pulp tissue-derived CD31⁻;CD146⁻ SP cells can be added. It provides advantages for clinical use, since autologous pulp tissue is easily available from useless teeth after extraction with no ethical issues.

CONCLUSION

Dental pulp-derived CD31⁻;CD146⁻ subfraction of SP cells is vasculogenic, and may induce vasculogenesis in vivo in the amputated pulp model. We are aware of the potential clinical

utility to ameliorate ischemic disease and pulp regeneration in the cell therapy for endodontics and operative dentistry.

DISCLOSURE OF POTENTIAL CONFLICTS OF INTEREST

The authors indicate no potential conflicts of interest.

REFERENCES

1 Takahashi T, Kalka C, Masuda H et al. Ischemia- and cytokine-induced mobilization of bone marrow-derived endothelial progenitor cells for neovascularization. Nature Med 1999;5:434–438.
2 Crosby JR, Kaminski WE, Schatteman G et al. Endothelial cells of hematopoietic origin make a significant contribution to adult blood vessel formation. Circ Res 2000;87:728–730.
3 Gehling UM, Ergun S, Schumacher U et al. In vitro differentiation of endothelial cells from AC133-positive progenitor cells. Blood 2000;95: 3106–3112.
4 Peichev M, Naiyer AJ, Pereira D et al. Expression of VEGFR-2 and AC133 by circulating human CD34(+) cells identifies a population of functional endothelial precursors. Blood 2000;95:952–958.
5 Taguchi A, Soma T, Tanaka H et al. Administration of CD34+ cells after

stroke enhances neurogenesis via angiogenesis in a mouse model. J Clin Invest 2004;114:330–338.
6 Alessandri G, Girelli M, Taccagni G et al. Human vasculogenesis ex vivo: Embryonal aorta as a tool for isolation of endothelial cell progenitors. Lab Invest 2001;81:875–885.
7 Zengin E, Chalajour F, Gehling UM et al. Vascular wall resident progenitor cells: A source for postnatal vasculogenesis. Development 2006; 133:1543–1551.
8 Miranville A, Heeschen C, Sengenes C et al. Improvement of postnatal neovascularization by human adipose tissue-derived stem cells. Circulation 2004;110:349–355.
9 Gronthos S, Brahim J, Li W. Stem cell properties of human dental pulp stem cells. J Dent Res 2002;81:531–535.
10 Pierdomenico L, Bonsi L, Calvitti M et al. Multipotent mesenchymal stem cells with immunosupressive activity can be easily isolated from dental pulp. Transplantation 2005;27:836–842.
11 Papaccio G, Graziano A, d'Aquino R, et al. Long-term cryopreservation

of dental pulp stem cells (SBP-DPSCs) and their differentiated osteoblasts: A cell source for tissue repair. J Cell Physiol 2006;208:319–325.

12 Iohara K, Zheng L, Ito M et al. Side population cells isolated from porcine dental pulp tissue with self-renewal and multipotency for dentinogenesis, chondrogenesis, adipogenesis, and neurogenesis. STEM CELLS 2006;24:2493–2503.

13 Nakashima M. Dentin induction by implants of autolyzed antigen-extracted allogeneic dentin on amputated pulps of dogs. Endod Dent Traumatol 1989;5:279–286.

14 Couffinhal T, Silver M, Zheng LP et al. Mouse model of angiogenesis. Am J Pathol 1998;152:1667–1679.

15 Ito M, Yoshioka M. Regression of the hyaloid vessels and pupillary membrane of the mouse. Anat Embryol 1999;200:403–411.

16 Asahara T, Murohara T, Sullivan A et al. Isolation of putative progenitor endothelial cells for angiogenesis. Science 1997;275:964–967.

17 Garmy-Susini B, Varner JA. Circulating endothelial progenitor cells. Br J Cancer 2005;93:855–858.

18 Reyes M, Dudek A, Jahagirdar B et al. Origin of endothelial progenitors in human postnatal bone marrow. J Clin Invest 2002;109:337–346.

19 Bardin N, Frances V, Lesaule G et al. Identification of the S-Endo 1 endothelial-associated antigen. Biochem Biophys Res Commun 1996;218:210–216.

20 Bardin N, George F, Mutin M et al. S-Endo 1, a pan-endothelial monoclonal antibody recognizing a novel human endothelial antigen. Tissue Antigens 1996;48:531–539.

21 Hristov M, Weber C. Endothelial progenitor cells: Characterization, pathophysiology, and possible clinical relevance. J Cell Mol Med 2004;8:498–508.

22 d'Aquino R, Graziano A, Sampaolesi M et al. Human postnatal dental pulp cells co-differentiate into osteoblasts and endotheliocytes: A pivotal synergy leading to adult bone tissue formation. Cell Death Differ 2007;14:1162–1171.

23 Gandia C, Arminan A, Gracia-Verdugo JM et al. Human dental pulp stem cells improve left ventricular function, induce angiogenesis, and reduce infarct size in rat with acute myocardial infarction. STEM CELLS 2008;26:638–645.

24 Grunewald M, Avraham I, Dor Y et al. VEGF-induced adult neovascularization: Recruitment, retention, and role of accessory cells. Cell 2006;124:175–189.

25 Yamamura T. Differentiation of pulpal cells and inductive influences of various matrices with reference to pulpal wound healing. J Dent Res 1985;64:530–540.

26 Tran-Hung L, Mathieu S, About I. Role of human pulp fibroblasts in angiogenesis. J Dent Res 2006;85:819–823.

27 Mathieu S, El-Battari A, Dejou J et al. Role of injured endothelial cells in the recruitment of human pulp cells. Arch Oral Biol 2005;50:109–113.

28 Roberts-Clark DJ, Smith AJ. Angiogenic growth factors in human dentine matrix. Arch Oral Biol 2000;45:1013–1016.

29 Lee M, Aoki M, Kondo T et al. Therapeutic angiogenesis with intramuscular injection of low-dose recombinant granulocyte-colony stimulating factor. Arterioscler Thromb Vasc Biol 2005;25:2535–2541.

30 Seiler C, Pohl T, Wustmann K et al. Promotion of collateral growth by granulocyte-macrophage colony-stimulating factor in patients with coronary artery disease: A randomized, double-blind, placebo-controlled study. Circulation 2001;104:2012–2017.

31 Buschmann IR, Busch HJ, Mies G et al. Therapeutic induction of arteriogenesis in hypoperfused rat brain via granulocyte-macrophage colony-stimulating factor. Circulation 2003;108:610–615.

32 Schneeloch E, Mies G, Busch HJ et al. Granulocyte-macrophage colony-stimulating factor-induced arteriogenesis reduces energy failure in hemodynamic stroke. Proc Natl Acad Sci U S A 2004;101:12730–12735.

33 Bergers G, Brekken R, McMahon G et al. Matrix metalloproteinase-9 triggers the angiogenic switch during carcinogenesis. Nat Cell Biol 2000;2:737–744.

34 Heissig B, Hattori K, Dias S et al. Recruitment of stem and progenitor cells from the bone marrow niche requires MMP-9 mediated release of kit-ligand. Cell 2002;109:625–637.

35 Cheng XW, Kuzuya M, Nakamura K et al. Mechanisms underlying the impairment of ischemia-induced neovascularization in matrix metalloproteinase 2-deficient mice. Circ Res 2007;100:904–913.

36 Renault MA, Losordo DW. The matrix revolutions: Matrix metalloproteinase, vasculogenesis, and ischemic tissue repair. Circ Res 2007;100:749–750.

37 Hashimoto G, Inoki I, Fujii Y et al. Matrix metalloproteinases cleave connective tissue growth factor and reactivate angiogenic activity of vascular endothelial growth factor 165. J Biol Chem 2002;277:36288–36295.

38 Sage EH, Reed M, Funk SE et al. Cleavage of the matricellular protein SPARC by matrix metalloproteinase 3 produces polypeptides that influence angiogenesis. J Biol Chem 2003;278:37849–37857.

39 Kupatt C, Horstkotte J, Vlastos GA et al. Embryonic endothelial progenitor cells expressing a broad range of proangiogenic and remodeling factors enhance vascularization and tissue recovery in acute and chronic ischemia. FASEB J 2005;19:1576–1578.

40 Young PP, Vaughan DE, Hatzopoulos AK. Biologic properties of endothelial progenitor cells and their potential for cell therapy. Prog Cardiovasc Dis 2007;49:421–429.

See www.StemCells.com for supplemental material available online.

膵島移植拒絶反応とNKT細胞

Novel roles of NKT cells in rejection of pancreatic islet transplantation

安波洋一
Yoichi YASUNAMI
福岡大学医学部再生・移植医学講座

◎著者らは膵島移植の研究を通して, NKT 細胞の異種, 同種ならびに自然免疫拒絶反応における役割を明らかにしている. いずれも臨床膵島移植の課題を解決し, 成績向上をめざすトランスレーショナルリサーチの成果である. とくに NKT 細胞が関与する自然免疫拒絶反応の研究は, 現在の臨床膵島移植が直面する課題, 移植膵島障害の新規制御法開発に直結し, 臨床膵島移植のブレイクスルーとなる可能性がある. 今後の方向性として, 膵島移植に関連して NKT 細胞の内因性リガンド発見を含めた NKT 細胞活性化機序の解明をめざし, 研究を進めている.

Key word ナチュラルキラー T(NKT)細胞, インスリン依存糖尿病, 膵島移植, 拒絶反応

インスリン依存糖尿病(insulin-dependent diabetes mellitus：IDDM)の新規治療法として, 膵島移植の臨床応用が開始されている[1]. 膵島移植は細胞移植であり, 侵襲の少ない治療法として今後の発展が期待されているが, 解決すべき課題は多い. 現在の臨床膵島移植でもっとも重要な課題は細胞移植特有の拒絶反応による移植膵島障害の制御であり, そのメカニズム解析に基づく治療法開発が求められている. 著者らは, 膵島移植部位(肝)の免疫担当細胞の解析より, NKT 細胞を介したあらたな拒絶反応機序, ならびにその制御法を見出した. 本稿では, 膵島移植拒絶反応における NKT 細胞の役割と今後の方向性について言及する.

インスリン依存糖尿病と移植医療

IDDM は, 生体内で唯一の血糖降下ホルモンであるインスリンを産生する細胞である膵島 β 細胞の欠落によって発症する疾患であり, インスリンを注射で投与する治療法が行われている. しかし, インスリン治療では十分な血糖管理ができず, 治療に難渋する例がある. とくに低血糖が問題で,

発汗, 手指振戦, 頭痛などの低血糖症状を自覚できない病態, 自律神経障害による突然の低血糖意識障害により, 生命予後に重大な影響を及ぼすことがある. さらには血糖管理が不十分な状態が長期に持続すると, 合併症(網膜症, 腎症, 神経症)を発症する.

このような IDDM を対象としてインスリン産生細胞の移植が行われる(「サイドメモ」参照). 膵島 β 細胞には血糖に対するセンサーがあり, 血糖を生理的範囲に調節している. したがって, インスリン産生細胞を移植すると移植膵島が血糖調節を行い, レシピエントの血糖は移植後ただちに正常となり, 低血糖発作は消失, さらには合併症の防止, 改善が期待できる.

膵島移植の実際と課題

膵島移植は欧米では脳死ドナー, わが国では心停止ドナーより提供された膵臓より膵島を単離し, 移植に用いられる. 移植の実際は, 局所麻酔下, 超音波ガイド下に肝臓内血管(門脈)を穿刺, カテーテルを留置し, 点滴の要領でドナー膵島を
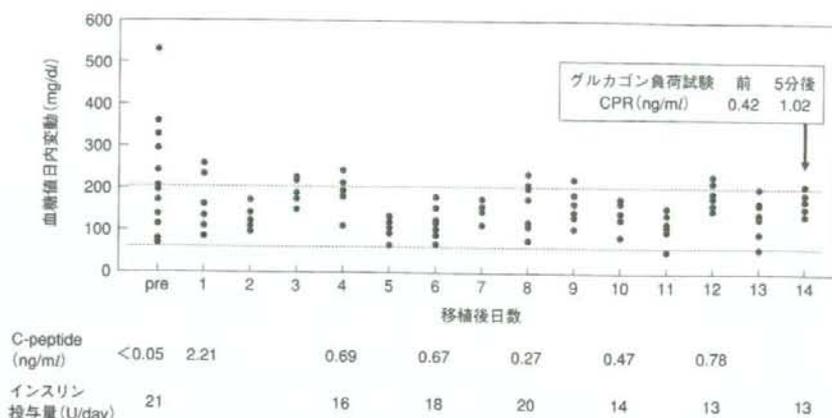
図 1　福岡大学症例の膵島移植後臨床経過
　移植前には測定感度以下であったレシピエント血中 C-ペプチドが膵島移植直後より認められ、血糖
値はほぼ正常範囲となっている. また, 負荷試験による C-ペプチド上昇は移植膵島が機能しているこ
とを示している.

注入(移植)する. 移植膵島は, 門脈末端に塞栓後
生着, 機能する. その結果, レシピエントの血糖

　インスリン産生細胞移植には膵臓器移植と膵島細胞
移植がある. ヒトの膵臓は重さ約 100 g で 100 万個の
膵島が存在する. 1 個の膵島は大きさ平均(径)150〜
250μM で約 2,000〜3,000 個の細胞からなり, その
60〜70%がインスリン産生(β)細胞である. 重要な点
は, 膵島は膵臓の約 1〜2%(容積)を占めるにすぎず,
98%以上は外分泌細胞である. このように, 膵臓器移
植では 1〜2%の膵島を移植するために膵臓全体を移
植している. 一方, 目的とする膵島のみを取り出し移
植に用いるのが膵臓細胞移植である. 膵臓器移植は全
世界で 2 万例以上行われ, すでに確立した医療となっ
ている. 膵島移植は 1973 年, Lacy らにより糖尿病が
膵移植により根治できることがはじめて実験的に明
らかにされ, 臨床応用への研究が開始された. 著者は
1980 年に Lacy 研に加わり, 臨床膵島移植を目的とし
た大動物膵島単離法の開発を進めた. 1990 年に同グ
ループにより第一例目の膵島移植が実施され, 2000 年
になり, カナダのグループにより膵島移植の成功例が
報告された. わが国では現在まで 18 例の膵島移植が行
われ, 2004 年に京大グループが第一例目を, 福岡大学
では 2006 年に実施した.

は移植直後より正常範囲となり安定する[1](図 1).
しかし, インスリン治療より離脱するには, 引き
続き 2〜3 回の移植, すなわち 2〜3 人のドナーが
必要である[1]. さらには移植膵島機能は残存してい
るものの, 時間の経過とともに再度インスリン治
療が必要になる[2].

　膵島移植レシピエントの解析より, 健常人と同
等数の膵島移植を受けたにもかかわらず, 移植膵
島の 36%しか生着していないことが判明し, 何ら
かの原因で早期より移植膵島が障害され, 喪失し
ていることが示された. このように臨床膵島移植
の現在のもっとも重要な課題は, 移植膵島障害の
機序を解明し, あらたな治療法を見出すことにあ
るといっても過言ではない.

移植膵島障害とNKT細胞

　移植膵島障害の成因としては, 同種拒絶反応,
自己免疫拒絶反応, 免疫抑制剤であるカルシ
ニューリンインヒビター(FK506, cyclosporine A)
による膵島(β細胞)障害などがよく知られている
が, 著者らは移植早期の自然免疫による膵島障害
に着目し, あらたな移植膵島障害の機序, ならび
に制御法を見出した[3].
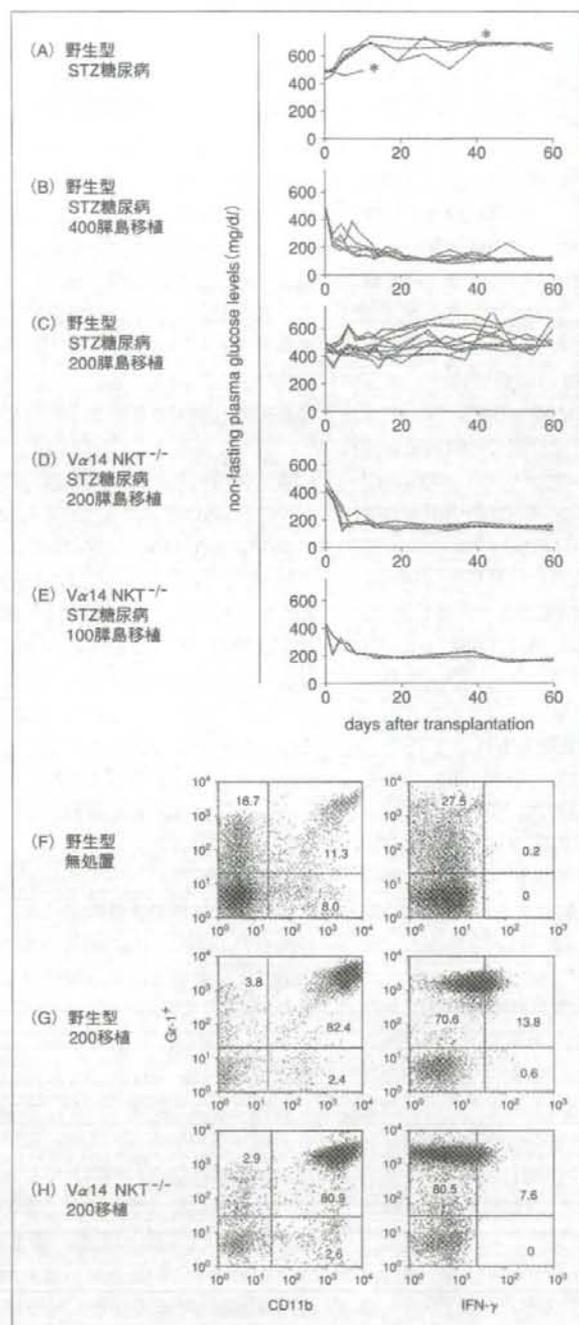
　膵島移植は細胞移植であるがゆえに, 種々の部
位に移植可能である. 臨床膵島移植ではインスリ

図 2 移植膵島障害におけるNKT細胞の役割
　ストレプトゾトシン糖尿病マウス(C57BL/6)を作成し，膵島移植レシピエントに用いた(A)．同種同系単離膵島を野生型(B：400 個，C：200 個)，あるいは Vα14⁻ᐟ⁻マウス(D：200 個，E：100 個)の経門脈的肝内移植した．膵島 200 個移植 6 時間後の野生型(G)または Vα14NKT⁻ᐟ⁻(H)マウスより肝単核球を単離し，FACS で解析した．

ンが生理的に第1に肝臓に灌流する，局所麻酔で容易に移植できる，動物実験で効果が確認できているなどにより，肝臓が移植部位として選択され，ドナー膵島は経門脈的肝内に移植される．移植後に膵島は門脈末端に塞栓し，末梢側肝臓に虚血性変性が生じ，それに伴い炎症などの自然免疫反応が惹起され，移植膵島が破壊される．とくに肝臓は生体防御の第一線臓器として機能しており，強い自然免疫反応が起こりうる．

著者らは，その際に肝臓内に豊富に存在するNKT細胞が移植膵島障害に関与しているのではないかと想定した．その仮説を直接的に検証するために，Vα14 NKT細胞欠損マウス[4]を実験に使用した．ストレプトゾトシン糖尿病野生型マウス（C57BL/6）の経門脈的肝内に同種同系マウス1匹分の膵島200個を移植した場合，移植後レシピエントの血糖は正常化せず，高血糖で推移した（図2-C）．一方，2匹分400個の膵島移植後には正常血糖になった（図2-B）．このことはマウスにおいてもヒトと同様に，1匹の糖尿病レシピエントを膵島移植後にインスリン離脱するには2匹のドナーが必要であることを示している．驚いたことに，糖尿病Vα14 NKT細胞欠損マウスをレシピエントに用いた場合，200個（図2-D）のみならず100個（図2-E）の膵島移植で血糖は正常化した．さらに，細胞移入の実験においてもVα14 NKT細胞が移植早期膵島障害に必須の役割を担っていることが明らかになった．

FACS解析で，膵島移植後6時間の野生型マウス肝臓内にはIFN-γを産生するCD1dαGalCer-tetramer^{+}CD3^{+}（NKT）細胞が出現，さらにはIFN-γ^{+}Gr-1^{+}CD11b^{+}細胞が肝内に集積することが判明した（図2-G）．さらには200個の膵島移植レシピエントに抗Gr-1抗体，抗CD11b抗体，あるいは抗IFN-γ抗体を投与すると移植後正常血糖になった．Vα14 NKT細胞欠損マウスへの移植後では，Gr-1^{+}CD11b^{+}細胞が野生型と同様に肝内に集積するものの，IFN-γ産生はみられなかった（図2-H）．以上の知見は，NKT細胞に依存したGr-1^{+}CD11b^{+}細胞によるIFN-γ産生が移植早期膵島障害に必須の役割を果たしていることを示している．

つぎに，NKT細胞の合成リガンドであるα-galactosylceramide（α-GalCer）[5]を用い，NKT細胞を標的にした治療法を試みた．NKT細胞はα-GalCerの1回投与でIFN-γを大量に放出するが，繰り返し投与後にはIFN-γ産生は抑制されることが知られている．野生型糖尿病マウスに移植前α-GalCerを繰り返し投与（−15，−10，−7d）し，ストレプトゾトシンで糖尿病作成後に200個の膵島を移植すると血糖は正常化した．これらの知見は，NKT細胞を標的にした治療法で移植早期膵島障害が制御できることを示している．

移植免疫におけるNKT細胞の役割

NKT細胞にはエフェクター細胞，ならびに調節性細胞としての機能があることが報告されている[6]．著者らは移植免疫におけるNKT細胞の機能について解析し，マウス肝臓内CD4^{+}NKT細胞が調節性細胞としてラットからマウスへの異種膵島移植拒絶反応の制御にかかわっていることを明らかにした[7]．また，マウス同種膵島移植ではNKT細胞は拒絶反応の発現に関与しており，NKT細胞欠損マウスでは野生型と比較してグラフトの長期生存が得られることを報告した[8]．

今後の展望

臨床膵島移植の成績向上には，マウス実験系で得られた成果がヒトに応用できるかどうかを見極めることが急務と考え，現在ヒト肝リンパ球を用いた in vitro 実験系で検討している．さらに，著者らが見出したNKT細胞を介した移植膵島障害の機序をもとに，臨床ですでに使用されている薬剤で制御できるものがないか，マウス実験系でスクリーニングしている．その結果，現在までにいくつかの有望な薬剤が判明しており，現在その臨床導入を検討している．また，著者らは膵島移植を通して，NKT細胞の動態・機能を解析してきたが，今後の研究によりいまだ明らかではないNKT細胞の内因性リガンドの発見につながる可能性があるのではないかと考え，研究を進めている．